Analyst

ROYAL SOCIETY OF CHEMISTRY

TUTORIAL REVIEW

View Article Online
View Journal | View Issue

Check for updates

Cite this: *Analyst*, 2022, **147**, 2338

Electrochemiluminescent sensor based on an aggregation-induced emission probe for bioanalytical detection

Xiaoyi Lv, [a] Yanping Li,[a] Bo Cui, [a] Yishan Fang *[a] and Lishi Wang[b]

Received 28th February 2022,
Accepted 14th April 2022

DOI: 10.1039/d2an00349j

rsc.li/analyst

In recent years, with the rapid development of electrochemiluminescence (ECL) sensors, more luminophores have been designed to achieve high-throughput and reliable analysis. Impressively, after the proposed fantastic concept of "aggregation-induced electrochemiluminescence (AIECL)" by Cola, the application of AIECL emitters provides more abundant choices for the further improvement of ECL sensors. In this review, we briefly report the phenomenon, principle and representative applications of aggregation-induced emission (AIE) and AIECL emitters. Moreover, it is noteworthy that the cases of AIECL sensors for bioanalytical detection are summarized in detail, from 2017 to now. Finally, inspired by the applications of AIECL emitters, relevant prospects and challenges for AIECL sensors are proposed, which is of great significance for exploring more advanced bioanalytical detection technology.

Published on 14 April 2022. Downloaded on 2/20/2026 8:42:33 PM.

1 Introduction

Various biological molecules, such as biomarkers,[1,2] toxins,[3,4] small biological molecules,[5,6] metal ions,[7] nucleic acid[8] and others[9,10] play crucial roles in our daily lives, and their excessive or too low presence could lead to severe threats to human health. Therefore, the precise and selective detection of these biological molecules has attracted widespread attention recently. Electrochemiluminescence (ECL) refers to emitters being oxidized or reduced to generate excited species with higher energy, which could be released in the form of light while returning back to the ground state.[11,12] It is a unique luminescence phenomenon, where light can be excited without any external excitation source, and a lower background signal observed, which is a major superiority over fluorescence (FL).[13] Therefore, ECL biosensors with good controllability, easy operation and sensitive detection have currently received more interest in the field of biological detection.[14–16] It is worth noting that the optical properties of the luminophore have a significant effect on the sensor, so some defects in ECL probes, such as pollution of the target, poor biocompatibility and lower quantum yield, could impede the development of biosensors.[17,18] Consequently, the design of a non-toxic, efficient, easy to synthesize and functionalized biological probe is of great significance for ECL biosensors.

The aggregation-induced emission (AIE) phenomenon refers to weaker light being observed in dilute solution, while stronger light could be emitted in the aggregate state or solid film, which was first discovered by Tang's group in 2001.[19,20] Most traditional organic light-emitting molecules with a large planar π-conjugated structure display a severe quenching effect in high concentration or the polymerization state due to intermolecular π–π stacking, which is a typical aggregation-caused quenching effect (ACQ).[21,22] Unlike the traditional ACQ, AIE molecules often have a non-coplanar structure.[23] The proposed AIE overcomes the self-quenching effect of conventional luminescent materials and, moreover, an extended luminous life and more stable light could be observed.[24] Since then, particularly in recent years, this major discovery has opened up a new path for biochemical analysis, and appealing emitters are widely used in detection, imaging and physiotherapy, and this brings about promising prospects for biosensors. Of course, more fields for its application need to be explored.[25–27]

Aggregation-induced electrochemiluminescence (AIECL) refers to a phenomenon where an illuminant could emit an extremely weak ECL signal in a good solvent, while an obviously enhanced ECL signal is obtained in a poor solvent, which combines the advantages of AIE material and ECL technology.[28] This is mainly attributed to the restricted molecular motion in a poor solvent, in which the energy leakage of the excited state molecules is blocked effectively, and more energy could be consumed in the form of light during the process of relaxation.[29] In 2017, Cola's team reported the

[a]*State Key Laboratory of Biobased Material and Green Papermaking, School of Food Science and Engineering, Qilu University of Technology, Shandong Academy of Sciences, Jinan, 250353, China. E-mail: fangysh123@qlu.edu.cn*
[b]*School of Chemistry and Chemical Engineering, South China University of Technology, Guangzhou 510641, People's Republic of China*

This journal is © The Royal Society of Chemistry 2022

Published on 14 April 2022. Downloaded on 2/20/2026 8:42:33 PM.

electrochemiluminescence properties of a square planar Pt(II) complex with a supramolecular nanostructure, and found that the aggregated Pt(II) complex could perform stronger ECL emission than the separated form, which is mainly induced by the different energy gap between the highest occupied molecular orbital (HOMO) and lowest unoccupied molecular orbital (LUMO) in the self-assembly process. As a result, the novel term "aggregation-induced electrochemiluminescence" was proposed.[30]

Biocompatibility in aqueous media and the complex diversity of detection environments still is a major challenge for organic materials in bioanalysis. However, after the proposed notion of AIECL, emitters with the AIECL property inject new possibilities for bioanalytical detection and application by ECL sensors. Especially in the solid state, this has greatly solved the compatibility problem between the illuminator and the biological medium in the ECL sensor, and effectively reduced the background interference simultaneously and, as a result, it has significantly enhanced the detection sensitivity.[31] Afterwards, more probes with the AIECL property in ECL sensors have been reported, and huge potential and broad application prospects are expected.

2 AIE emitters

2.1 Principle of AIE emitters

Regarding the AIE phenomenon, restricted intramolecular motion (RIM), including restricted intramolecular rotation (RIR) and restricted intramolecular vibration (RIV), is recognized as a common principle to explain the AIE mechanism by most researchers.[32]

2.1.1 Restricted intramolecular rotation (RIR). As a typical AIE molecule, hexaphenylsilole (HPS) with a propeller structure performs as a non-coplanar structure, which consists of six freely rotatable benzene rings and a central axis of a silole molecule (Fig. 1A).[33] A larger amount of energy could be consumed in solution owing to the strong molecular motion of the benzene ring rotor, and weaker light is observed. Whereas, in the aggregate state, the intermolecular accumulation and spatial physical restraint extremely limit the free rotation of the rotor, and the non-radiative attenuation channel is blocked and, thereby, a strong light is emitted when the excited molecule returns to the ground state.

2.1.2 Restricted intramolecular vibration (RIV). With the in-depth study of the AIE phenomenon, another theory of RIV was proposed owing to pure RIR theory not being explain the light emission of more AIE molecules, such as (Fig. 1B) 10,10′,11,11′-tetrahydro-5,5′-bidibenzo[*a*,*d*][7]annulenylidene (THBA) with a flexible ethyl chain and tetraphenylethylene (TPE) with four peripheral aromatic phenyl rings and a central olefin stator.[33,34] Similarly, the flexible part of the THBA molecule vibrates strongly in a good solvent, huge energy is liberated through the non-radiative transition channel, and weak light is observed. The blocked movement of the molecule promotes more energy to be released in the form of light in the aggregate state.

Some other mechanisms, such as molecular conformation,[35] J-aggregate formation,[36] *E*/*Z* isomerization,[37] excited-state intramolecular proton transfer[38] and twisted intramolecular charge transfer[39] can also be employed to help explain the AIE phenomenon; however, they are all lack systemicity and universality to a certain extent.[40]

2.2 Novel AIE emitters

In addition to traditional AIE materials such as TPE and HPS, researchers have tried to design various AIE molecules with excellent optical properties, and many new AIE emitters have been synthesized, such as TPE derivatives,[41] phenylenevinylene derivatives,[42] silacyclopentadienes[43] and fluorenonearylamine derivatives *etc*.[44] In general, AIE emitters are mainly divided into the following several categories: small organic molecule AIEgens, organic macromolecular AIEgens, AIEgen bioconjugates, metal-containing AIEgens and AIE polymers.

Since the first discovery of the small organic molecule AIEgens in 2001, various AIE molecules with outstanding fea-

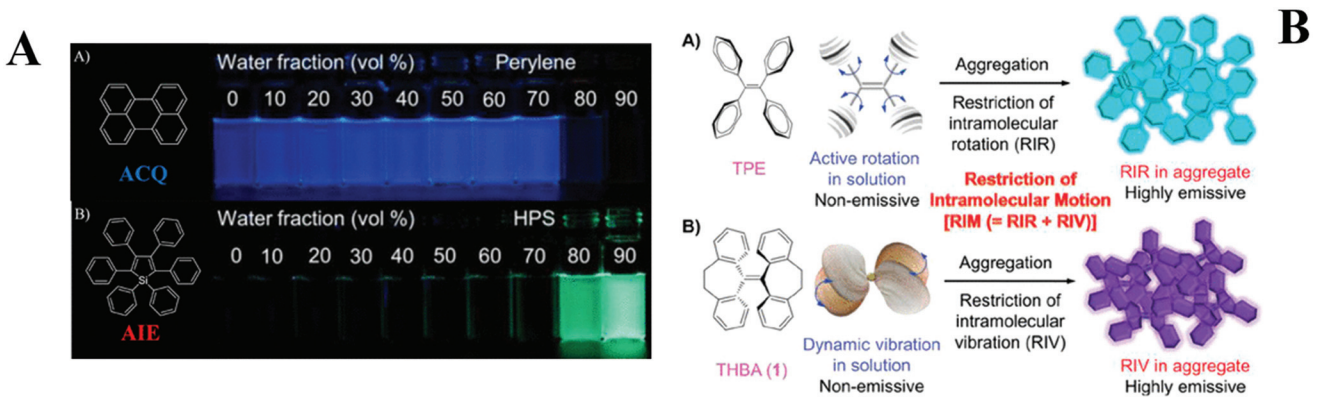

Fig. 1 Fluorescence of perylene and HPS in a mixture of THF/water with different fw (A). RIV and RIR behavior of TPE and THBA respectively. Adapted from (Wang *et al.* 2020) with permission of *Chemical Reviews*, copyright 2020 (B).

Published on 14 April 2022. Downloaded on 2/20/2026 8:42:33 PM.

tures have been designed through the introduction of different substituents or other methods, and they were successfully applied in biosensors.[45] Yuan designed a small molecule AIEgen (named TPY) through the reaction of 3-ethyl-2-methylbenzothiazol-3-ium bromide (an electron acceptor) and TPE-CHO (an electron donor). Bright orange fluorescence can be observed without hypochlorite, and then transformed to blue in the presence of hypochlorite. The transition of this color is mainly due to the oxidation of the ethylene bridge; therefore, the sensor achieved an effective distinguishing of hypochlorite through the significant conversion in color.[46]

Compared with the small molecular AIEgens, it is much easier to adjust the structure, morphology and topology for macromolecular AIEgens, in which the part of the AIE unit could be introduced into a limited space, such as a metal–organic framework (MOF) or covalent organic framework (COF), or embedded in the chains or backbones of macromolecular AIEgens.[47–49] As a typical example, a TPE@γ-CD-MOF-K complex was prepared through *in situ* encapsulation, and the porous structure of γ-CD-MOF provides more paths to encapsulate guest TPE molecules, and the fluorescence signal of the complex is stronger than that of pure TPE molecules due to the limited movement of TPE in the MOF. Impressively, nitroaromatic compounds could be detected through specific recognition between K^+ and nitro compounds.[50]

An AIE bioconjugate is an emitter in which different biomolecules, such as amino acids, nuclei acids, proteins and others, could interact with AIE molecules through specific covalent linkages.[51] For example, Yu recently synthesized AIE emitter 4*H*-pyrimido-[2,1-*b*]benzothiazoles with different substitutions through the Biginelli reaction, and the fluorescence signal could be adjusted by diverse substitutions. In the presence of bovine serum albumin (BSA), a higher signal could be observed due to the limited intramolecular motion. A prepared sensor based on this excellent strategy performed good detection for human serum albumin (HAS).[52] Metal-containing AIEgens are competitive candidates for an effective ECL emitter. For example, a Tb-based MOF was reported by introducing the AIE-active molecule TPE, where the intramolecular motion could be suppressed due to the embedded AIE unit in the rigid MOF matrix, which significantly improved the ECL efficiency. Thus a highly selective "turn-off" sensor was proposed for CrO_4^{2-}, $Cr_2O_7^{2-}$ and Fe^{3+} detection, in which an obvious quenching effect was observed with an increase in the target.[53]

As for an AIE polymer, it could perform with better optical properties due to its aggregation characteristics.[54] Very recently, Zhang synthesized a supramolecular AIE polymer (PT-G), which emitted yellow light in the aggregate state. Then PT-GEu and PT-GTb were prepared through the coordination effect between Eu^{3+}, Tb^{3+} and PT-G, respectively. Amazingly, a "turn-off" light was obtained with the introduction of Eu^{3+} and Tb^{3+}, while a "turn-on" light was observed under exposure to CN^- and ClO_4^-, which is attributed to the specific interactions between Eu^{3+} and CN^-, Tb^{3+} and ClO_4^-.[55]

3 AIECL emitters

Up to now, as a new detection method, ECL sensing technology has developed rapidly, and a series of remarkable achievements have been obtained owing to its lower noise, faster detection and higher sensitivity.[56–58] Since different illuminants could directly determine the performance of the sensor platform, some ECL emitters with insolubility, toxicity and poor stability greatly limit the development of ECL sensors.[59–61] Therefore, the preparation of ECL emitters with higher luminous efficiency and stability is essential.

Currently, organic illuminants have become popular in ECL sensors due to their well designable structure, abundant variety and high biocompatibility.[62,63] Han designed a porphyrinic Zr metal–organic framework, PCN-224, and achieved sensitive detection for porcine epidemic diarrhea virus with the assistance of TiO_2 NPs, which acted as an accelerator and promoted the generation of more $SO_4^{\bullet-}$, thereby resulting in a higher ECL signal.[64]

Du *et al.* prepared CdSQDs@MOF-5 through encapsulating CdS quantum dots (CdSQDs) into MOF-5, which emitted two ECL signals under different potentials. Then a potential resolved multicolor electrochemiluminescence system was constructed through the intensity difference between these two ECL signals.[65] Also, very recently, lanthanide metal–organic frameworks (LMOFs) with a self-luminescent property were reported. The designed emitter with excellent ECL performance provides guidance for research into new ECL illuminators.[66]

In order to take full advantage of the unique properties of organic ECL emitters, further types of ECL emitters were developed. It is worth mentioning that the rapid development of AIECL emitters endows unprecedented activity for ECL sensors after the proposed concept of AIECL by Cola's group in 2017. Over the last five years, much effort has been paid to developing different kinds of AIECL luminophores, which have been applied to AIECL sensors, and effectively solved the problem between signal intensity and biocompatibility in ECL sensors.

Recently, Xu *et al.* designed a series of iridium(III)-containing polytetraphenylethene Pdots (PTPE Pdots), and discussed their different ECL properties through capping or embedding the iridium complexes into the TPE chain. The results showed that the end-capped copolymer suffered less damage to the polymer backbone during the synthesis process, and promoted rapid intramolecular electron transfer and, therefore, a higher ECL signal was obtained. The relative ECL efficiency of the end-capping copolymer was calculated to be 18.9% compared with $Ru(bpy)_3^{2+}$/tri-*n*-propylamine (TPrA). This suggests a new idea for the design of ECL emitters with brighter light.[67]

In addition, Carrara reported a redox metallopolymer based on a cyclometalated iridium(III) center, where the iridium redox center was decorated onto the polymer backbone. After modifying the polymer on the electrode surface, a thin film was formed, and a strong AIECL signal was emitted due to the protected iridium metal center. The designed Ir(III)-based polymers obtained higher ECL efficiency and resolved the solubi-

 This journal is © The Royal Society of Chemistry 2022

Published on 14 April 2022. Downloaded on 2/20/2026 8:42:33 PM.

lity problem in aqueous media for the iridium(III) complex, so the obtained emitter displayed significant advantages for a solid ECL sensor.[68]

4 The construction strategy of AIECL sensors

The effective and precise regulation of the luminescence properties of AIECL molecules is an important part of designing and constructing highly sensitive sensors towards various biomolecules. Common construction strategies for AIECL sensors are as follows (Fig. 2).[69]

4.1 Target-mediated specific binding

Very recently, Lu and co-workers designed a series of tetraphenylbenzosilole derivatives with an AIECL property based on the intermolecular radical cyclization reaction of diphenylacetylenes and triphenylsilane, among which 2,3-bis(4-cyanophenyl)-1,1-diphenyl-benzosilole (TPBS-C) displayed the highest ECL efficiency (184.36%), which is mainly attributed to the obstructed non-radiative transition of aggregated molecules and the lowest reduction potential of TPBS-C with electron-withdrawing cyano groups. In this system, the sensor performed a "turn-off" response toward Cr^{4+} due to the strong oxidation property of $Cr_2O_7^{2-}$, and the target could capture electrons in the reduction of TPBS-C, and a decreased ECL signal was obtained (Fig. 3A).[70]

4.2 Self-assembly

An AIECL sensor could be constructed through self-assembly, such as electrostatic interaction, hydrogen bonding, hydrophobic effects and coordination/chelation *etc*. Interestingly, Jiang proposed a hydrogel network composed of gold nanoclusters, which could be connected with Ca^{2+}. The prepared hydrogel network performed excellent AIECL emission, with 50-fold ECL enhancement. Finally, the AIECL signal of this sensor was induced towards calmodulin through a specific combination between calmodulin and the Ca^{2+} linker (Fig. 3B).[71]

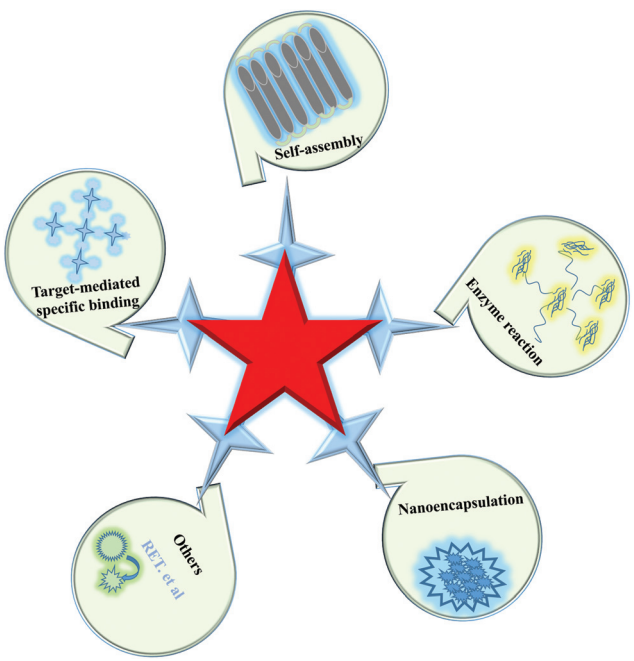

Fig. 2 Common construction strategies for AIECL sensors.

4.3 Reaction with enzymes

Reactions with enzymes could facilitate the cleavage or dissolution of ligands to form or dissolve aggregates. Very recently, Li *et al.* reported a phosphate-containing TPE with the AIECL property. The AIEgens could emit a strong anode signal with the assistance of coreactant TEA. In the presence of target ALP, the phosphate group of the AIEgens could be decomposed, and a decreased ECL signal would be observed (Fig. 3C).[72]

4.4 Nanoencapsulation

Apoferritin (apoFt) with a cavity of 8 nm can serve as a host to encapsulate a guest molecule and form bioconjugates with the AIECL property. Very recently, Wei and his colleagues synthesized an $Ir(ppy)_3$@apoFt bioconjugate through wrapping *fac*-tris(2-phenylpyridine)iridium(III) complexes into the apoFt cavity. About 44.3 molecules of $Ir(ppy)_3$ were encapsulated in apoFt through intermolecular π–π stacking interactions and hydrogen bonds. The restricted space with nano-encapsulation greatly hindered the intramolecular movement of the AIE molecule. In aggregates, the ECL signal of $Ir(ppy)_3$@apoFt was 5.3-fold stronger than in the monomers. The emergence of this novel AIE bioconjugate provides a new method for the design of more AIE molecules (Fig. 3D).[73]

4.5 Other construction strategies

For example, Wang *et al.* prepared AIE-active Pdots through a Suzuki reaction between TPE and boron ketoiminate. Then, the prepared Pdots were decorated with ssDNA and used to specifically recognize UO_2^{2+} through the coordinate bonds of P=O and U between the phosphonate groups. The ECL signal was apparently enhanced with more UO_2^{2+}, which is attributed to the resonance energy transfer (RET) mechanism from UO_2^{2+} to Pdots.[74]

Although the development of AIECL sensors is in its infancy, it exhibits unique advantages in the fields of clinical diagnosis, biomarker detection, and environmental and food analysis, especially in biosensors.

5 Application of AIECL illuminants in biosensors

AIECL-based biosensors have developed rapidly since the introduction of AIECL emitters in recent years, which have been employed to detect various targets accurately through specific identification features, such as hydrogen bonding or a

Published on 14 April 2022. Downloaded on 2/20/2026 8:42:33 PM.

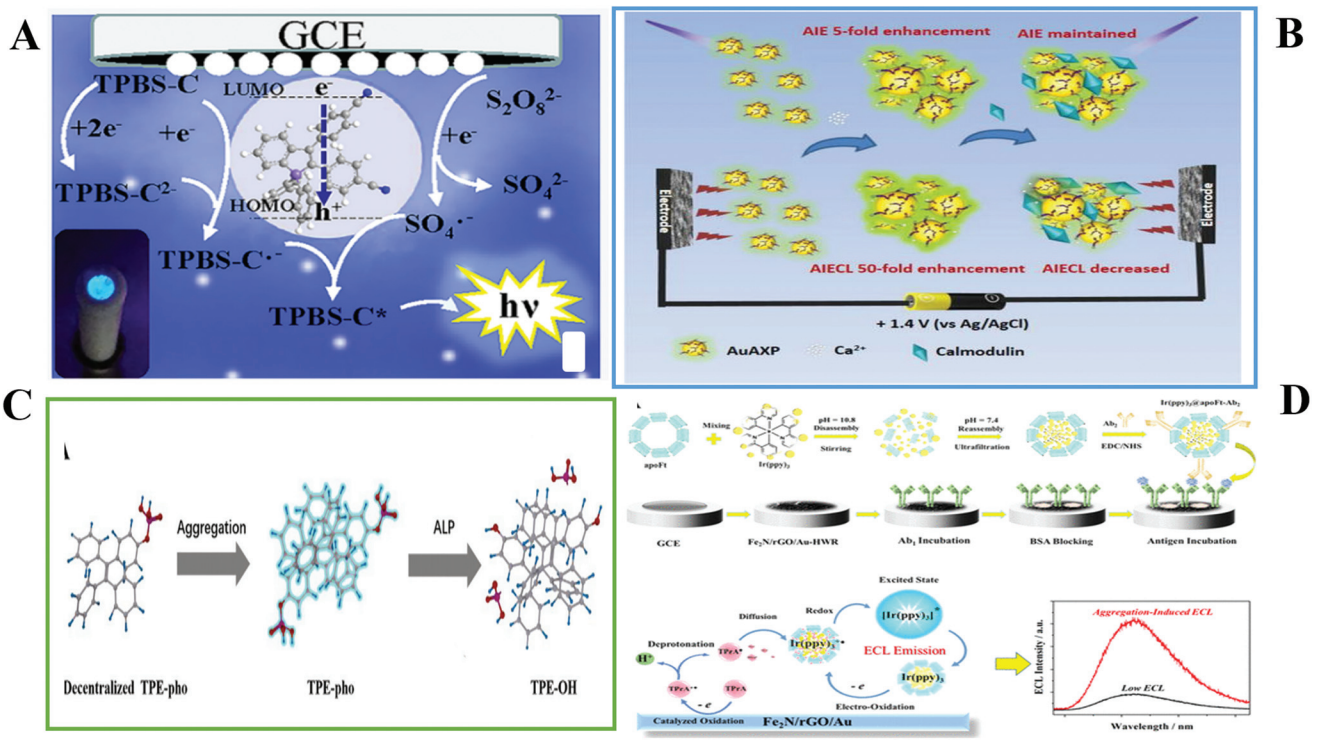

Fig. 3 The mechanism of a designed ECL sensor towards its target. Adapted from (Guo *et al.* 2020) with permission of *Analytical Chemistry*, copyright 2020 (A). Construction of an AIECL sensor for calmodulin detection. Adapted from (Jiang *et al.* 2019) with permission of *Small*, copyright 2019 (B). Detection principle of a designed ECL sensor for ALP. Adapted from (Li *et al.* 2021) with permission of *Microchemical Journal*, copyright 2021 (C). Assembly process of an ECL sensor based on Ir(ppy)$_3$@apoFt for CYFRA 21-1 detection. Adapted from (Yang *et al.* 2021) with permission of *Analytical Chemistry*, copyright 2021 (D).

hydrophobic effect.[75] The remarkable cases of AIECL sensors for biological analysis are shown in the following section (Fig. 4).

5.1 Application in protein markers

Protein markers are important biochemical indicators, which could be used to mark structural or functional changes in organs, tissues, cells and subcellular structures in our bodies due to their unique sensitivity.[76,77] The sensitive and accurate detection of a variety protein markers could provide early prevention of many diseases.

As a traditional tumor marker, the abnormal expression of mucin 1 (MUC1) in tumor tissue is closely related to canceration.[78] Recently, Yuan designed an exquisite sensing platform based on the strategy of "restriction of intramolecular motions-driven ECL". In this system, hexagonal tetraphenylethylene microcrystals (TPE MCs), as an aggregate state of the TPE molecule, displayed the strongest ECL signal at 675 nm in a poor solution, which was 12.7 times higher than that of the TPE monomer. This is the result of the physical constraint. Then, palladium nanospheres were used to capture Fc-labeled substrate DNA in the sensor, and a "signal-off" model was developed. After capturing MUC1, the Fc-labeled DNA fragments were released into solution, and a "signal-on" signal could be realized (Fig. 5A).[79] Afterwards, Xiao *et al.* fixed a

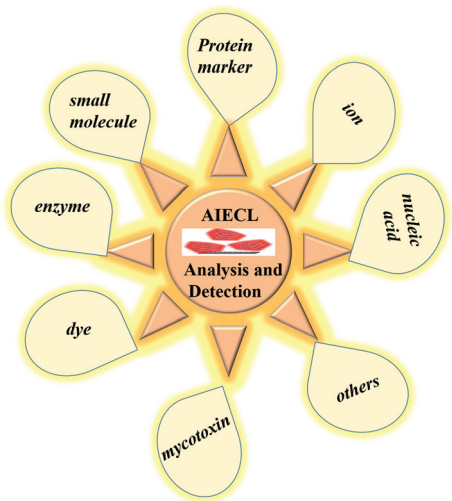

Fig. 4 The main applications of AIECL emitters in bioanalytical testing.

TPE-based ligand with MOF to design a novel ECL emitter (Hf-TCBPE), where the enrichment and concentration effect of the MOF greatly shortens the distance of ion/electron-transfer between the emitter and co-reactant, resulting in brighter light signals. As a result, Hf-TCBPE achieved excellent performance for MUC1 detection.[80]

 This journal is © The Royal Society of Chemistry 2022

Published on 14 April 2022. Downloaded on 2/20/2026 8:42:33 PM.

Wei proposed a dumbbell-plate-like MOF with AIECL properties due to a coordination effect between 1,1,2,2-tetra(4-carboxylbiphenyl)ethylene (H_4TCBPE) and Zr(IV) cations. In this, more H_4TCBPE molecules were fixed in the MOF and, moreover, the abundant porous structure of the MOF activated the H_4TCBPE ligands, which existed in internally and at the surface of the MOF, and a powerful ECL signal was emitted. Additionally, coreactant polyethyleneimine (PEI) was covalently linked on the MOF to prepare Zr-TCBPE-PEI, which performed self-enhanced ECL due to the intramolecular coreaction acceleration effect. Then, the ECL signal was effectively quenched through the RET of quencher AuPd@SiO_2. The well-prepared ECL sensor was applied for neuron-specific enolase (NSE) detection through the "on–off" mode (Fig. 5B).[81]

As a typical tumor marker, the detection of cytokeratin 19 fragment 21-1 (CYFRA 21-1) is of great significance. Wei synthesized an Ir(ppy)$_3$@apoFt bioconjugate with AIECL characteristics as a probe. On the other hand, reduced graphene oxide modified by Fe_2N and gold nanoparticles was prepared, and functioned as an electroactive substrate to accelerate the reaction of free radicals. Therefore, this ECL immunosensor for CYFRA 21-1 performed good detection with a limit of 0.43 pg mL^{-1}.[73] Similarly, the same team proposed another AIECL emitter, TP-COOH NCs, which were prepared through wrapping poly-(styrene-*co*-maleicanhydride) onto tetraphenylethylene nanocrystals. An ECL sensor for CYFRA 21-1 was fabricated based on TP-COOH NCs and iron-doped hydroxyapatite (Fe-HAP), and the effective energy level matching and good spectral overlap between TP-COOH NCs and Fe-HAP improved the detection of CYFRA 21-1.[82]

Acute myocardial infarction (AMI) is one of the most threatening cardiovascular diseases, and troponin I (TI) is an important biological indicator of AMI. Recently, Saremi's group fabricated a disposable aptasensor for TI based on the deposition of cyclometallated iridium(III)-polyvinylpyridine polymer nanoparticles (CIPNPs) on nitrogen-doped graphene, where the sensor was assembled gradually through nitrogen-doped graphene (NG), AuNPs-Apt and CIPNPs. More importantly, CIPNPs showed higher ECL intensity in the aggregate state compared with Ru(bpy)$_3^{2+}$. In this system, ECL intensity increased with increasing target concentration due to the specific recognition of TI and aptamer, and the well-designed aptasensor was perfectly utilized to detect TI in sample serum (Fig. 5C).[83]

The effective detection of M.SssI methyltransferase (M.SssI MTase) is of great significance in clinical diagnosis and research. It is worth mentioning that very recently Cui *et al.* designed Ag-metal–organic gels (Ag-MOG) as an illuminant. Inspired by the host–guest recognition of ferrocene (Fc) and β-CD, a facile biosensor was constructed for M.SssI MTase detection. In the absence of the target, double-stranded DNA (dsDNA) formed from two single-stranded DNAs (biotinylated

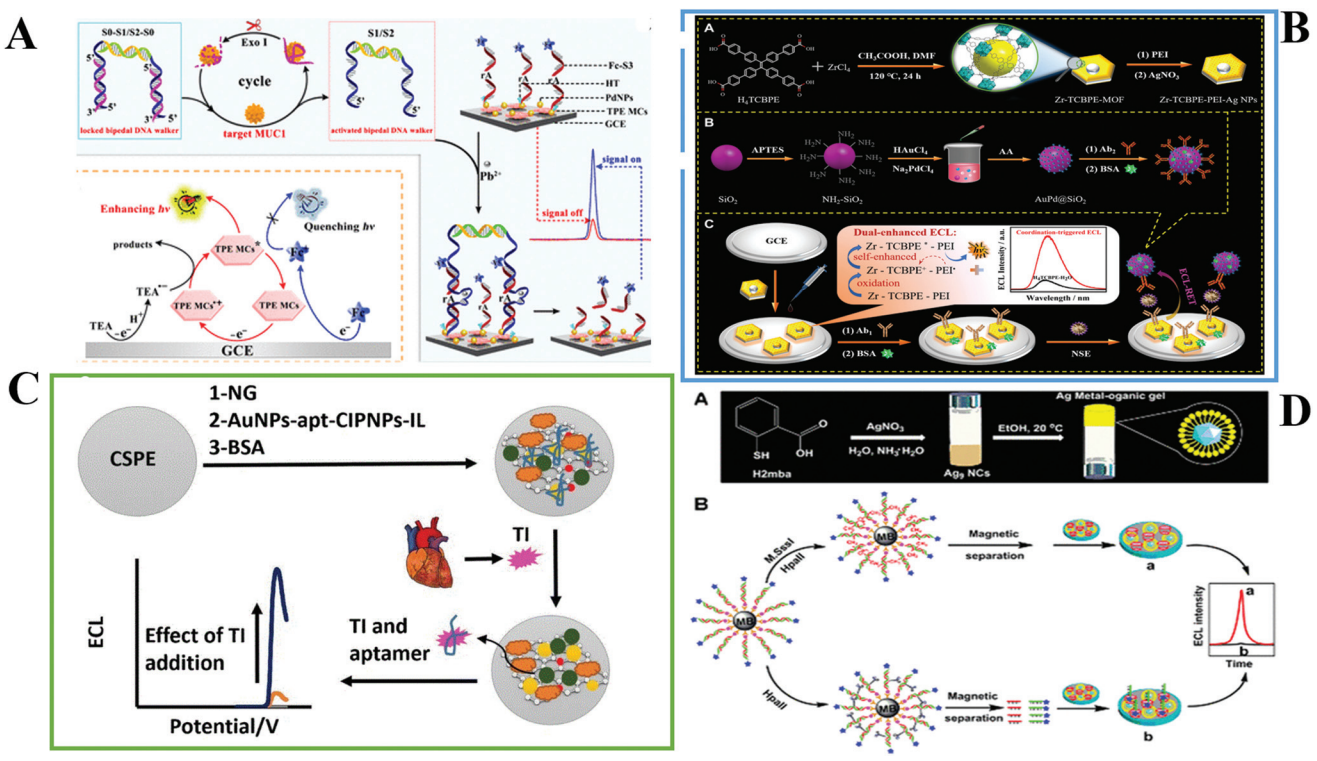

Fig. 5 Assembly process of an ECL sensor based on TPE MCs. Adapted from (Jiang *et al.* 2019) with permission of *Analytical Chemistry,* copyright 2019 (A). A designed sensor based on Zr-TCBPE-PEI for NSE detection. Adapted from (Li *et al.* 2022) with permission of *Small*, copyright 2022 (B). The manufacture of an ECL sensor. Adapted from (Saremi *et al.* 2019) with permission of *Microchimica Acta*, copyright 2019 (C). ECL sensor based on Ag-MOG for M.SssI MTase. Adapted from (Cui *et al.* 2021) with permission of *Analytical Chemistry,* copyright 2021 (D).

Published on 14 April 2022. Downloaded on 2/20/2026 8:42:33 PM.

DNA-1 and Fc-labeled DNA-2) was hydrolyzed by the restriction endonuclease HpaII. Then, Fc was liberated from the magnetic beads (MBs) and interacted with β-CD specifically, resulting in a quenched ECL signal. However, dsDNA could not be cleaved in the presence of M.SssI MTase, which blocked the division of Fc from MBs, and a higher ECL intensity was observed. The sensitive detection of the target is attributed to the fascinating supramolecular recognition system (Fig. 5D).[84]

Moreover, Yang reported a distyrylarylene derivative, 4,4′-bis (2,2-diphenylvinyl)-1,1′-biphenyl (DPVBi), and then prepared a solid-state high-efficiency ECL system for cTnI detection. Compared with typical tetraphenylethylene and its derivatives, a more stable and powerful ECL signal of DPVBi NBs was received, which is mainly due to the band gap emission.[85]

In addition, Jiang proposed a metal-binding protein responsive hydrogel with AIECL, which performed satisfying detection for calmodulin in the range of 0.3 to 50 μg mL^{-1}.[71] More ECL sensors based on AIECL emitters have been established for biomarker detection. All of these confirmed a promising outlook.[72,86,87]

5.2 Application in ions

Some ions such as Mg^{2+}, Ca^{2+}, Zn^{2+}, and Fe^{3+} are important to maintain healthy bodies, since they participate in normal physical activity in our daily lives. However, some toxic metal ions such as $Cr^{4+/3+}$, Pb^{2+}, Hg^{2+} and Cd^{2+} could induce metabolic disorders and generate fatal hazards.[88–91] AIECL emitters could be used as powerful probes in ECL sensors to detect these ions rapidly through unique interactions, such as metal-bridged crosslinking, chelation reaction, cleavage reaction and coordination effect *etc*.[92]

As one of the essential elements in our body, an abnormal content of Cu^{2+} could cause a series of diseases.[93] Fu *et al.* synthesized a J-aggregate, 5,10,15,20-tetrakis(4-carboxyphenyl) porphyrin (TCPP). Compared with the monomer, a 5-fold enhanced ECL signal for TCPP appeared at 675 nm. In order to further investigate the relevant ECL mechanism, density functional theory (DFT) calculations of the monomer and dimer (minimum aggregate) were carried out, where the narrower LUMO–HOMO band gap of the TCPP dimer effectively shortens the electron transfer distance, which is beneficial to the ECL emission of TCPP. Meanwhile, L-cysteine capped zinc oxide nanoflowers (ZnO@Cys NFs) were prepared, which played the roles of coreactant accelerator and energy donor. Thus, with resonance energy transfer (RET) from the ZnO@Cys NFs (energy donor) to the TCPP J-aggregate (energy acceptor), a solid-state detection platform was manufactured on the basis of the RET mechanism, and the proposed ECL sensor showed a highly selective and sensitive quenching effect for the detection of Cu^{2+} in the range of 1.0 pM to 500 nM (Fig. 6A).[94]

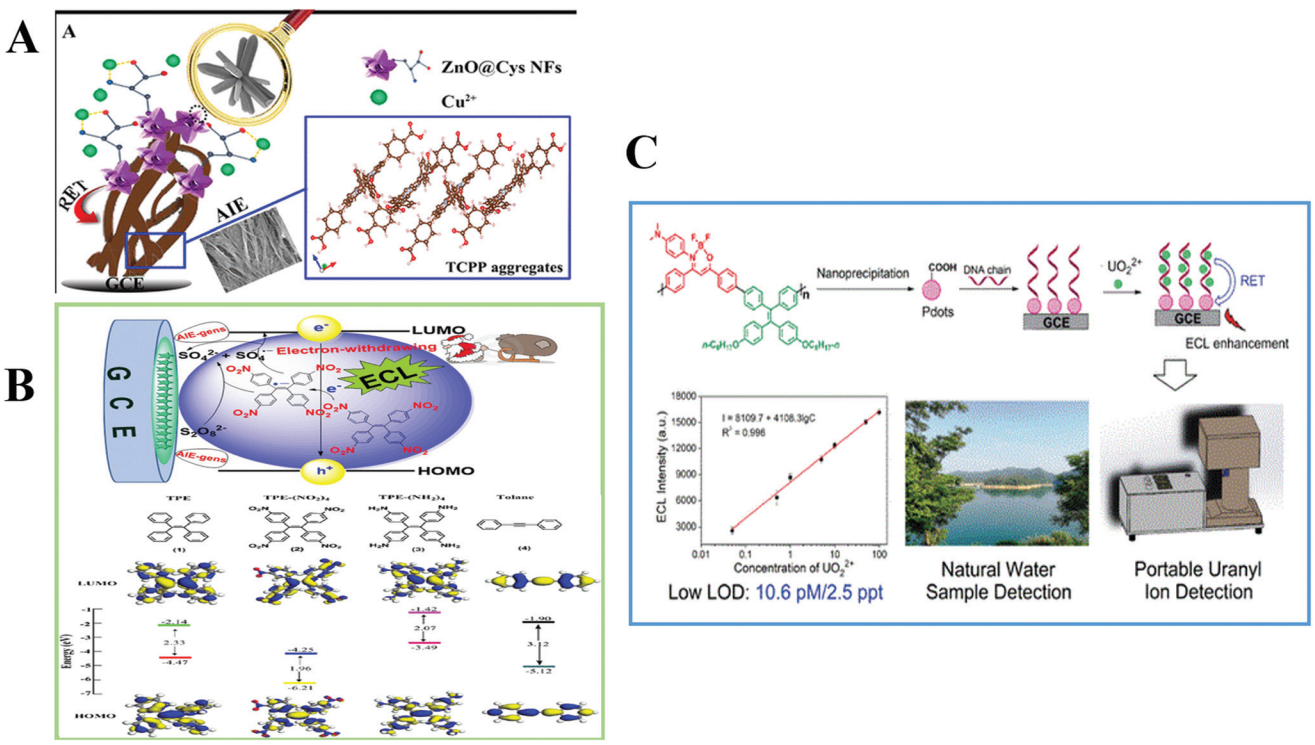

Fig. 6 Schematic illustration of an ECL sensor based on TCPP J-aggregate towards Cu^{2+}. Adapted from (Han *et al.* 2020) with permission of *Analytical Chemistry*, copyright 2020 (A). The mechanism of a designed ECL sensor, molecular orbital amplitude plots and the calculated orbital energy levels for TPE, TPE-$(NO_2)_4$, TPE-$(NH_2)_4$ and tolane molecules. Adapted from (Han *et al.* 2019) with permission of *Analytical Chemistry*, copyright 2019 (B). The assembly of a sensor for uranyl ions. Adapted from (Wang *et al.* 2020) with permission of *Advanced Functional Materials*, copyright 2020 (C).

 This journal is © The Royal Society of Chemistry 2022

Published on 14 April 2022. Downloaded on 2/20/2026 8:42:33 PM.

Recently, a series of different TPE derivatives were designed, and the important effects of different substituents in the organic compound for ECL emission were investigated through UV and electrochemistry analysis. Among them, TPE-$(NO_2)_4$/$K_2S_2O_8$ displayed the strongest ECL signal. It is worth noting that the ECL intensity increased with an increase in R/B absorbance band intensity ratios, and TPE-$(NO_2)_4$ exhibited the largest R/B ratio. In addition, DFT was used to study the effect of electronic structure on ECL emission. Analogous HOMOs appeared in these TPE derivatives, which is mainly attributed to the C=C bond, while a lower LUMO energy level appeared in TPE-$(NO_2)_4$, where the narrower LUMO–HOMO energy gap of TPE-$(NO_2)_4$ leads to easier electron transfer. All of these might be due to the strong electron-withdrawing group of $-NO_2$. Taking advantage of the powerful AIEgens, the as-prepared sensor based on TPE-$(NO_2)_4$/$K_2S_2O_8$ revealed sensitive detection towards iodide (Fig. 6B).[95]

In addition, Wang prepared an ECL-RET sensor for the detection of UO_2^{2+}, and the obtained LOD in this sensor is lower than for other methods (Fig. 6C).[74] Sun constructed a metal sensor based on three-component Pdots with an AIECL property, and obtained good detection for Pb^{2+}.[96]

5.3 Application in nucleic acids

Nucleic acid is indispensable for the construction of organisms, playing an extremely important role in genetics, mutation and protein biosynthesis.[97,98] Accurate detection of nucleic acids could assist clinical diagnosis at the level of gene expression.

Recently, Guo and his co-worker designed an AIECL-active dichlorobis(1,10-phenanthroline) ruthenium(II) ($Ru(phen)_2Cl_2$). The ECL and PL signals were obviously enhanced with an increment in the H_2O fraction (v%) from 30% to 70% in H_2O/MeCN media, increasing by 120 fold and 5.7 fold, respectively. In MeCN, the excited state molecules $Ru(phen)_2Cl_2$* interacted with each other or with the surrounding solvents, which consumed a large amount of energy in the process of non-radiative relaxation. With the addition of water, $Ru(phen)_2Cl_2$ molecules aggregated gradually due to weak intermolecular interaction, and the vibrational and rotational relaxation of $Ru(phen)_2Cl_2$* was restricted, resulting in a stronger light. Therefore, an ECL sensor based on the AIECL emitter was used to selectively identify miRNAs according to the type and number of different nucleobases (Fig. 7A).[99]

Afterwards, Zhang prepared active Pdots through a nanoprecipitation method, which are composed of a classical TPE derivate and benzothiadiazole (BT). BT with a hard frame and good electrochemical property could reduce damage to the conjugated structure of Pdots during the synthesis process, which is conducive to the generation of a stable ECL signal. Well-designed Pdots resolved the irreversible electric redox defect of general Pdots, and higher luminescence efficiency was observed in the aggregate state. Thus, a biosensor for

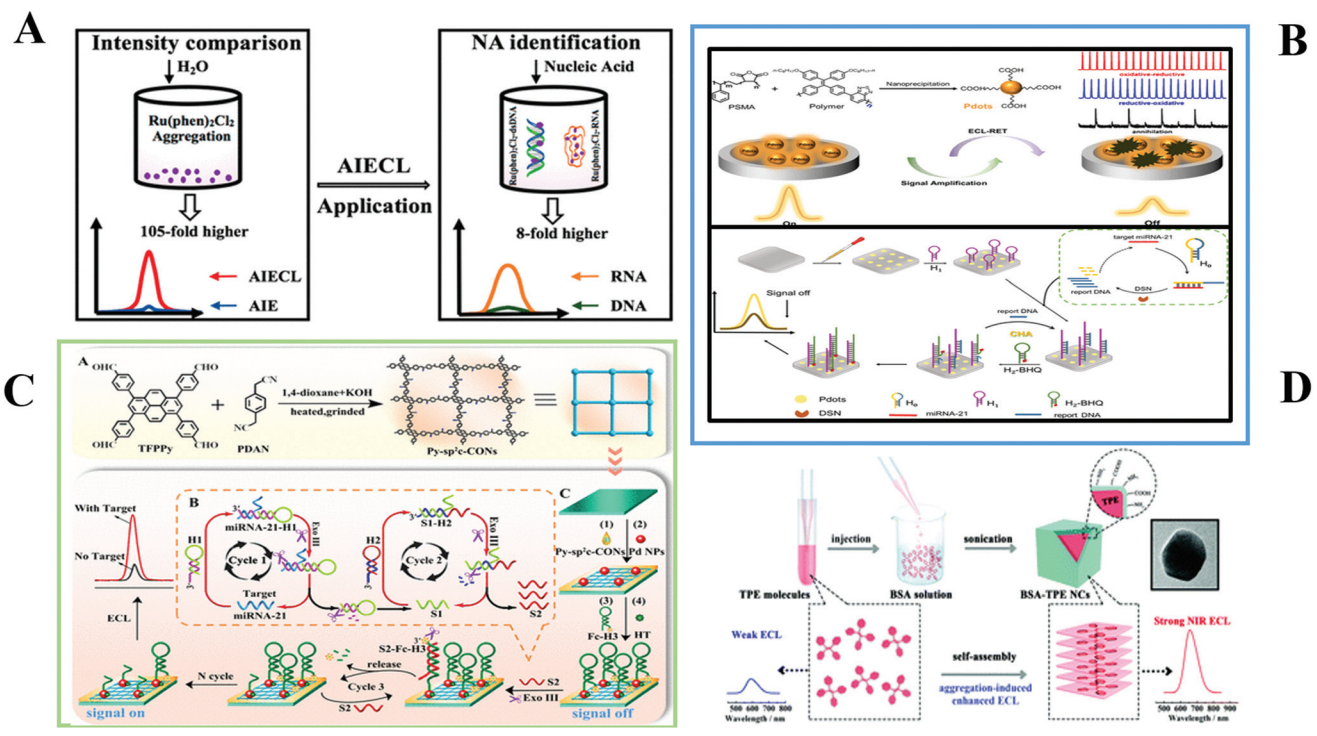

Fig. 7 AIECL of the $(Ru(phen)_2Cl_2)$/TPA system and its applications. Adapted from (Lu *et al.* 2020) with permission of *Analytical Chemistry*, copyright 2020 (A). Synthesis of active Pdots and the preparation of a sensor for miRNA-21. Adapted from (Zhang *et al.* 2021) with permission of *Analytical Chemistry*, copyright 2021 (B). Construction of a Py-sp^2c-CON emitter and a designed sensor for microRNA-21. Adapted from (Zhang *et al.* 2021) with permission of *Analytical Chemistry*, copyright 2021 (C). Assembly process of a sensor for microRNA. Adapted from (Liu *et al.* 2019) with permission of *Analytical Chemistry*, copyright 2019 (D).

Published on 14 April 2022. Downloaded on 2/20/2026 8:42:33 PM.

miRNA-21 detection was prepared based on target recycling amplification, a catalytic hairpin assembly method and an ECL-RET strategy (Fig. 7B).[100]

Very recently, Xiao's group designed a new pyrene-based sp^2 carbon-conjugated covalent organic framework nanosheet (Py-sp^2c-CON). This unique ultrathin nanosheet with large amounts of luminophores shortened the electron and ion transport channels, and further caused abundant excited state emitters, which significantly amplified the ECL signal. Subsequently, the accelerator $S_2O_8^{2-}$ further improved the ECL signal. As a result, an appealing probe was employed to construct a biosensor for microRNA-21 detection by using the strategy of *exo* III-assisted target recycling amplification (Fig. 7C).[101] Liu *et al.* also utilized BSA to stabilize tetraphenylethylene nanocrystals (BSA-TPE NCs), which showed excellent AIECL properties in the presence of triethylamine (TEA), and thus an ECL detection platform for microRNA based on BSA-TPE NCs was constructed (Fig. 7D).[102]

5.4 Application in small molecules

Many small molecules, such as dopamine, glucose and uric acid, are essential for the normal operation of life activities.[103–105] So, a variety of ECL sensors based on AIECL materials have been reported for the detection of these small molecules.

Chloramphenicol is a typical antibiotic, but many regions have forbidden its use due to its extremely toxic side effects, so the detection of chloramphenicol in food is essential for our health.[106] Luo's group synthesized a covalent organic framework with AIECL groups (COF-AIECL) based on the Schiff base reaction, which emitted a strong ECL signal under the coactivator H_2O_2. Moreover, a mercapto-modified Co_3O_4 nanozyme was synthesized, and the ECL intensity was significantly enhanced due to the catalytic effect of Co_3O_4 on H_2O_2. As a result, a novel molecularly imprinted chloramphenicol (CAP) sensor based on the signal element COF-AIECL, the amplification element Co_3O_4 and a recognition element molecularly imprinted polymer (MIP) was designed. The ECL signal was effectively controlled by the elution and adsorption of CAP. In this system, the detection of CAP in the range of 5×10^{-13} to 4×10^{-10} mol L^{-1} is satisfactory, with an LOD of 1.18×10^{-13} mol L^{-1} (Fig. 8A).[107]

Recently, Liang *et al.* reported a metal-free mass-amplifying electrochemiluminescence film (MAEF) based on a synthetic butterfly-shaped illuminator (BTD-TPA). The prepared MAEF is different from other reported ECL systems, and a linearly increased ECL signal could be observed with more modified

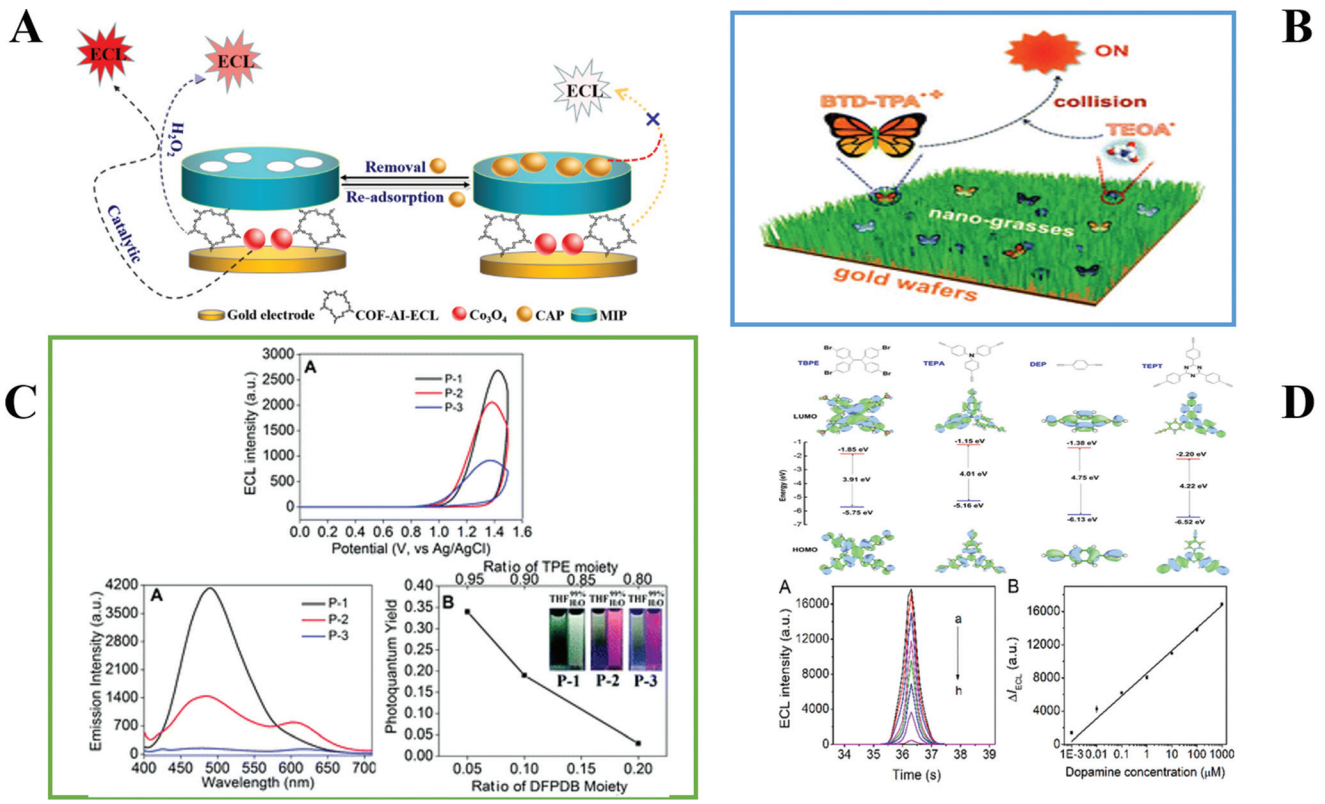

Fig. 8 Detection mechanism of a sensor for chloramphenicol. Adapted from (Li *et al.* 2021) with permission of *Biosensors and Bioelectronics*, copyright 2021 (A). A designed MAEF based on BTD-TPA for dopamine detection. Adapted from (Li *et al.* 2020) with permission of *Nanoscale*, copyright 2020 (B). Designed P-1 Pdots used for catechol, epinephrine and dopamine detection. Adapted from (Wang *et al.* 2020) with permission of *Analyst*, copyright 2020 (C). Synthesized TBPE-CMPs used for dopamine. Adapted from (Cui *et al.* 2020) with permission of *ACS Applied Materials and Interfaces*, copyright 2020 (D).

 This journal is © The Royal Society of Chemistry 2022

Published on 14 April 2022. Downloaded on 2/20/2026 8:42:33 PM.

MAEF on the Au-matrix. This is mainly due to the electrocatalytic effect of the Au substrate promoting the reaction of illuminant and coreactant; moreover, the nucleation centers of the Au-matrix are conducive to the growth of grass-like aggregates. The AIECL characteristics of BTD-TPA were verified in a tetrahydrofuran/water (THF/H_2O) mixture, where a sharply enhanced ECL signal was obtained with the increase in water. Besides this, orange-red light could be clearly observed. As a result, the prepared sensor was used for dopamine detection, and obtained a lower detection limit (3.3×10^{-16} M). This unique method provides a promising path for visual ECL imaging (Fig. 8B).[108]

Up to now, more research on donor–acceptor AIE luminophore has been reported. Wang prepared three Pdots (P-1, P-2 and P-3) through a Pd-catalyzed Suzuki coupling polymerization reaction, in which, a 9-octyl-3,6-bis(4,4,5,5-tetramethyl-1,3,2-dioxaborolan-2-yl)-9*H*-carbazole monomer (M2) was employed as an electron donor, and 4,6-bis((*E*)-4-bromostyryl)-2,2-difluoro-5-phenyl-2H-1l3,3,2l4-dioxaborinine (M3) was used as an electron acceptor, and the TPE unit played the role of an AIE-active moiety. The difference in these Pdots lies in the ratio of TPE units. Among them, P-1 Pdots performed with typical AIECL properties and emitted the strongest ECL intensity due to the highest ratios of TPE (0.95). Finally, a sensor based on P-1 Pdots was manufactured to detect catechol, epinephrine and dopamine (Fig. 8C).[109]

Afterwards, Cui *et al.* designed three conjugated microporous polymers (TBPE-CMPs) based on 1,1,2,2-tetrakis(4-bromophenyl)ethane (TBPE), where these polymers involved different conjugated ligands, and the different energy gaps generated in the TBPE-CMPs were used to adjust the electronic transition from the valence band to the conduction band, which promoted ECL emission to varying degrees. Among them, TBPE-CMP-1 was chosen to detect dopamine due to its better ECL emission, which is mainly caused by the enhanced electron–hole recombination efficiency. The ECL efficiency was computed to be 1.72% compared with $[Ru(bpy)_3]^{2+}$/TPrA. During the detection of dopamine, a linearly quenched ECL signal was obtained in the range of 0.001–1000 mM (Fig. 8D).[110]

Furthermore, Liu *et al.* designed donor–acceptor based coumarin derivatives, 6-[4-(*N*,*N*-diphenylamino)phenyl]-3-ethoxycarbonyl coumarin (DPA-CM), through a reprecipitation method, and the "oxidation–reduction" mechanism of TPrA and DPA-CM was verified by an electrochemistry study, where the constructed ECL sensor was used for the detection of ascorbic acid, uric acid and dopamine.[111] All of this demonstrated a fascinating analytical application of an AIECL sensor to small molecules.

In addition, Li reported a new AIECL emitter, a quaternary ammonium salt group-functionalized TPE derivate (QAU-1) with positive charge, and then QAU-1 was linked with Fc-labeled ssDNA based on electrostatic interaction. With an increase in the target, Fc molecules gradually fell off, and the ECL signal of the proposed sensor increased with the increment of BLM.[112]

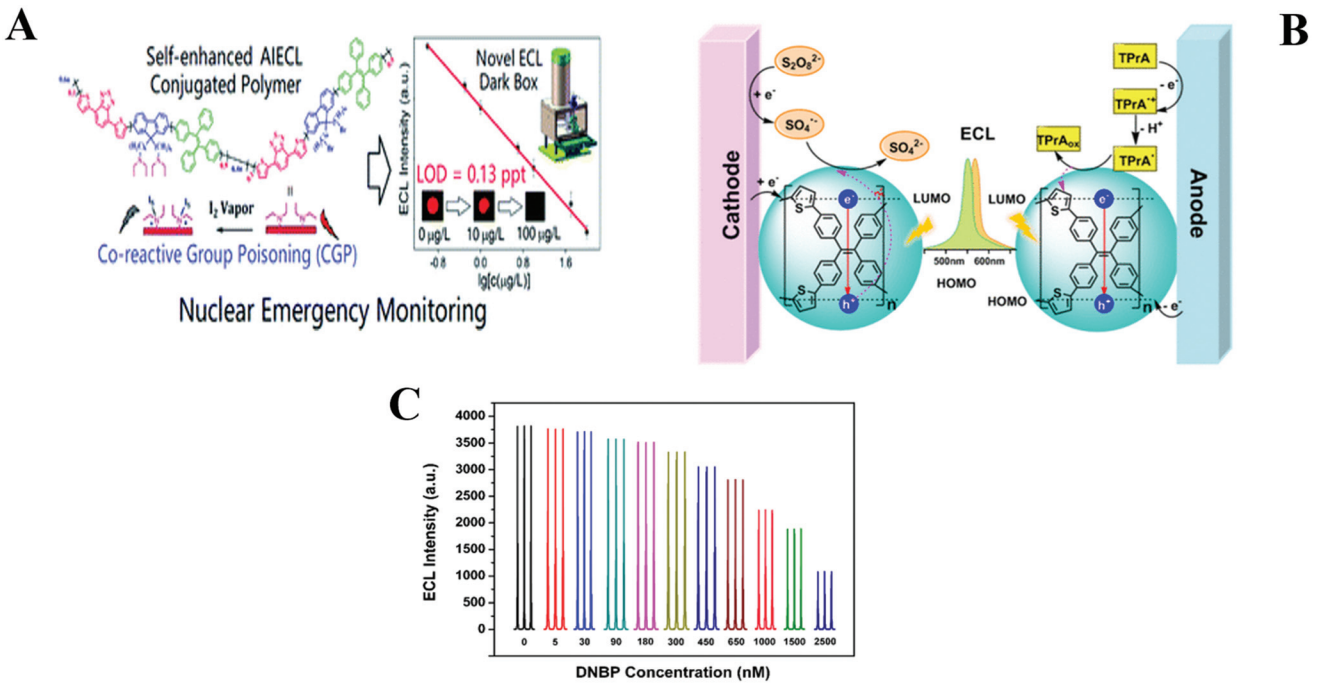

Fig. 9 A prepared AIECL sensor for I_2 vapour detection. Adapted from (Wang *et al.* 2021) with permission of *Journal of Materials Chemistry A*, copyright 2021 (A). A prepared AIECL sensor based on ThT-CMP for RhB detection. Adapted from (Cui *et al.* 2021) with permission of *ACS Applied Materials Interfaces*, copyright 2021 (B). A designed silole/$K_2S_2O_8$ system towards DNBP with various concentrations. Adapted from (Han *et al.* 2019) with permission of *Angewandte Chemie-International Edition*, copyright 2019 (C).

Published on 14 April 2022. Downloaded on 2/20/2026 8:42:33 PM.

As one of the most ordinary mycotoxins in nature, is aflatoxin B_1 (AFB1) widely scattered in animals and plants, and severe threat occurs every year owing to its hard-to-decompose and stable property.[113] Fang's group prepared novel 9,10-diphenylanthracene cubic nanoparticles (DPA CNPs) through a simple reprecipitation method, and a powerful ECL signal was observed in a mixture of water/*N*,*N*-dimethylformamide (DMF), because free intramolecular rotation and vibration are effectively limited in the aggregated state. In addition, the small size confinement effect could also enhance the emission of the ECL signal. Thus, a free-label sensor was prepared based on DPA CNPs, and acceptable detection was realized.[114]

5.5 Application in other aspects

Since the discovery of the AIECL phenomenon, a series of these new luminescent materials have been utilized in fields such as immunity, metal ion, nucleic acid and small molecule detection. Nowadays, they have also gradually attracted more attention in other fields.

I_2 radioisotopes have an important effect in the early warning of nuclear accidents, and bring heavy pressure on environmental governance. Wang reported a polymer with AIECL properties, which was decorated with tertiary amine as co-reactive groups; moreover, the tertiary amine plays a role as a vapor capturing and sensing group in an ECL sensor. This work is the first time it has been used to monitor radioactive I_2 vapour, which has a great potential for public security (Fig. 9A).[115]

Cui designed a thiophene tetraphenylethene-based conjugated microporous polymer (ThT-CMP), which could emit positive and negative ECL signals with the coreactants TPrA and $S_2O_8^{2-}$ at the same time. Then a dipolar AIECL sensor was prepared for rhodamine B (RhB) detection (Fig. 9B).[116]

Han *et al.* constructed a heterogeneous aggregation-induced emission ECL (HAIE-ECL) in the silole/$K_2S_2O_8$ system, which realized the sensing of organic-based ECL in the water phase by solving the crucial problem of water insolubility for the specific recognition of di-*n*-butyl *ortho*-phthalate (DNBP) plasticizer, and this strategy achieved satisfactory detection for DNBP (Fig. 9C).[117]

All the above cases illustrate the wide applications of AIECL illuminants in ECL biosensors, which provides a theoretical basis for future market development. And the representative examples of electrochemiluminescent sensors based on aggregation-induced emission probes for bioanalytical detection are shown in Table 1.

Table 1 Representative examples of electrochemiluminescent sensors based on aggregation-induced emission probes for bioanalytical detection

Target analyte	Sensing strategies	AIECL emitter (with coreactant)	Linear range	LOD	Ref.
Cr(VI)	Turn on	TPBS-C ($S_2O_8^{2-}$)	10^{-12} to 10^{-4} M	0.83 pM	70
Ca^{2+}	Turn off	AIECL-type hydrogel system TPE-pho (TEA)	0.3–50 μg mL^{-1}	0.1 μg mL^{-1}	71
ALP	Turn off	$Ir(ppy)_3$@apoFt bioconjugate (TPrA)	0.1–6.0 U L^{-1}	0.037 U L^{-1}	72
CYFRA 21-1	Turn on	Pdots (TPrA)	1 pg mL^{-1} to 50 ng mL^{-1}	0.43 pg mL^{-1}	73
Uranyl ion	Turn on	TPE MCs (TEA)	0.05 to 100 nm	10.6 pm/2.5 ppt	74
MUC1	Turn on	Zr-TCBPE-PEI	1 fg mL^{-1} to 1 ng mL^{-1}	0.29 fg mL^{-1}	79
NSE	Turn off	TP-COOH NCs ($S_2O_8^{2-}$)	0.0001 to 10 ng mL^{-1}	52 fg mL^{-1}	81
CYFRA 21-1	Turn off	CIPNPs (TPA)	10^{-7}–500 ng mL^{-1}	0.01471 pg mL^{-1}	82
TI	Turn on	MOG ($S_2O_8^{2-}$)	0.1 pM to 10 nM	20 fM	83
M.SssI MTase	Turn on	DPVBi NBs (TEA)	0.05 to 100 U mL^{-1}	3.5×10^{-3} U mL^{-1}	84
cTnI	Turn off	TCPP J-aggregate ($S_2O_8^{2-}$)	0–100 μg L^{-1}	43 fg mL^{-1}	85
Cu^{2+}	ECL–RET	TPE-$(NO_2)_4$ ($S_2O_8^{2-}$)	1.0 pM to 500 nM	0.33 pM	94
Iodide	Turn off	DPF (TEA)	5 to 2000 nM	0.23 nM	95
Pb^{2+}	Turn on	$Ru(phen)_2Cl_2$ (TPrA)	100 pM to 1.0 μM	38.0 pM	96
miRNAs	—	Pdots (TPrA)	—	—	99
miRNA-21	ECL–RET	Py-sp^2c-CON ($S_2O_8^{2-}$)	0.1 fM to 100 pM	32 : 00 : 00	100
microRNA-21	Turn on	BSA-TPE NCs (TEA)	100 aM to 1 nM	46 : 00 : 00	101
microRNA	Turn on	COF-AI-ECL (H_2O_2)	100 aM to 1 nM	13.6 aM	102
Chloramphenicol	Turn on	BDT-TPA (TEOA)	5×10^{-13} to 4×10^{-10} M	1.18×10^{-13} M	107
Dopamine	Turn off	P-1 Pdots (TPrA)	5×10^{-15} to 4×10^{-8} M	3.3×10^{-16} M	108
Datechol, dopamine and epinephrine	Turn off	TBPE-CMP-1 (TPrA)	2 nM to 1 mM, 10 nM to 100 μM and 10 nM to 500 μM	1, 7 and 3 nM	109
Dopamine	Turn on	QAU-1 ($S_2O_8^{2-}$)	0.001–1000 μM	0.85 nM	110
Bleomycin	Turn on	DPA CNPs (TPrA)	0.01 to 10 000 pM	4.64 fM	112
aflatoxin B1	Turn off	Conjugated polymer Pdots (TEA)	0.01 pg mL^{-1} to 100 ng mL^{-1}	3 fg mL^{-1}	114
I_2 vapor	Turn off	ThT-CMP (TPrA)	0–100 μg L^{-1}	0.13 ppt	115
RhB	Turn off	HPS ($S_2O_8^{2-}$)	0.0001 to 10 μM	0.055 nM	117
Plasticizers	Turn on		5–2500 nM	0.15 nM	117

 This journal is © The Royal Society of Chemistry 2022

Published on 14 April 2022. Downloaded on 2/20/2026 8:42:33 PM.

6 Conclusions and prospects

In this work, we introduced the phenomenon, principle and main applications of AIE and AIECL emitters. The applications of AIECL emitters in ECL sensors over the past five years were summarized. A variety of AIECL illuminants perform appealing properties, which opens a new avenue for the development of novel ECL biosensors. The proposed AIECL not only overcomes the notorious ACQ in the aggregate state or solid film, and greatly improves the sensing capability, but also solves the application restrictions of ECL sensors in aqueous or other media. Nowadays, ECL biosensors based on AIECL emitters are developing rapidly and performing with great potential due to their unique optical properties.

Up to now, only limited AIECL illuminators have been exploited in biosensors among the existing large number of AIE materials, and it is expected that there will be more abundant AIECL illuminant types. In order to obtain various AIECL illuminators and broaden the application of AIECL sensors, more methods for manipulating AIECL molecules need to be developed. AIE bioconjugates have received more attention due to their better water solubility and biocompatibility in biosensors, especially in the biomedical field. For example, AIE bioprobes based on enzyme-responsive peptides perform with excellent specificity and have potential value. The enzymatic hydrolysis of a peptide can induce the aggregation of AIE molecules, which could be used to detect enzymatic activities closely related to some diseases. This has been widely applied in fluorescence analysis but rarely reported in ECL sensors recently.[118]

On the other hand, while AIECL emitters are employed in many detection systems, most exhibit a "turn-off" detection mode, where the quenching effect is enhanced with increasing target, and a gradually decreased ECL signal could be observed. This type of sensor is very susceptible to interference from various components, and false detection can appear. In contrast, the "light-up" detection based on AIE materials has attracted a lot of attention in the field of bioanalytical detection due to its unique advantages. In particular, the target can induce the formation of aggregates through hydrogen bonding, electrostatic attraction, coordination cyclization and target-induced charge transfer *etc.*, resulting in an opened ECL emission. This target-induced "signal-on" mode partially avoids the decreased ECL signal due to nonspecific binding.

Additionally, the original design of the AIECL emitter has a huge number of vacancies; therefore, it is very promising to design a novel AIECL emitter with a stable structure and a lower redox potential, which could significantly reduce the damage to biomolecules. Finally, in AIECL-based biosensor systems, it is also essential to find more coreactants that could match with the AIECL molecules. With the advancement of microarray technology and the development of AIECL illuminators, the miniaturization of biosensors is expected to be realized quickly and applied in practical applications. Although the development of these sensors is in its initial stage, it is an emerging and attractive research field.

Conflicts of interest

The authors have read the policy on conflicts of interest and declare no competing interests with other people or organization.

Acknowledgements

We are deeply grateful for the support of National Natural Science Foundation of China (No. 21705084), the Natural Science Foundation of Shandong Province of China (No. ZR2017BB074), the National Training Program of Innovation and Entrepreneurship for Undergraduates (No. S202010431027), Qilu University of Technology of Training Program of Innovation and Entrepreneurship for Undergraduates (No. xj201910431125), the Research Leader Workshop of Jinan (2021GXRC101), the Key Research and Development Program of Shandong Province (No. 2021CXGC010808), the Innovation Team of Jinan City (2018GXRC004), and the Special Funds for Taishan Scholars Project.

References

1 Y. Zeng, J. Bao, Y. N. Zhao, D. Q. Huo, M. Chen, Y. L. Qi, M. Yang, H. B. Fa and C. J. Hou, A sandwich-type electrochemical immunoassay for ultrasensitive detection of non-small cell lung cancer biomarker CYFRA21-1, *Bioelectrochemistry*, 2018, **120**, 183–189.

2 D. M. Qin, X. H. Jiang, G. C. Mo, J. S. Feng, C. H. Yu and B. Y. Deng, A novel carbon quantum dots signal amplification strategy coupled with sandwich electrochemiluminescence immunosensor for the detection of CA15-3 in human serum, *ACS Sens.*, 2019, **4**, 504–512.

3 W. D. Wu, H. R. Zhou and J. J. Pestka, Potential roles for calcium-sensing receptor (CaSR) and transient receptor potential ankyrin-1 (TRPA1) in murine anorectic response to deoxynivalenol (vomitoxin), *Arch. Toxicol.*, 2017, **91**, 495–507.

4 L. Liu, Q. W. Huang, Z. L. Tanveer, K. Q. Jiang, J. H. Zhang, H. Y. Pan, L. J. Luan, X. S. Liu, Z. Han and Y. J. Wu, "Turn off-on" fluorescent sensor based on quantum dots and self-assembled porphyrin for rapid detection of ochratoxin A, *Sens. Actuators, B*, 2020, **302**, 127212.

5 N. N. Song, Y. Z. Wang, X. Y. Yang, H. L. Zong, Y. X. Chen, Z. Ma and C. X. Chen, A novel electrochemical biosensor for the determination of dopamine and ascorbic acid based on graphene oxide/poly (aniline-co-thionine) nanocomposite, *Electroanal. Chem.*, 2020, **873**, 114352.

6 W. T. Chiu, T. F. M. Chang, M. Sone, A. T. Mita and H. Toshiyoshi, Electrocatalytic activity enhancement of Au NPs-TiO_2 electrode via a facile redistribution process

Published on 14 April 2022. Downloaded on 2/20/2026 8:42:33 PM.

towards the non-enzymatic glucose sensors, *Sens. Actuators, B*, 2020, **319**, 128279.
7 Y. H. Wang, X. L. Pan, Z. Peng, Y. H. Zhang, P. Liu, Z. X. Cai, B. Tong, J. B. Shi and Y. P. Dong, A "turn-on" fluorescent chemosensor with the aggregation-induced emission characteristic for high-sensitive detection of Ce ion, *Sens. Actuators, B*, 2018, **267**, 351–356.
8 Y. Xiong, J. J. Zhang, Z. L. Yang, Q. B. Mou, Y. Ma, Y. H. Xiong and Y. Lu, Functional DNA regulated CRISPR-Cas12a sensors for point-of-care diagnostics of non-nucleic-acid targets, *J. Am. Chem. Soc.*, 2020, **142**, 207–213.
9 A. Kaushika, P. R. Solanki, A. A. Ansari, B. D. Malhotra and S. Ahmad, Iron oxide-chitosan hybrid nanobiocomposite based nucleic acid sensor for pyrethroid detection, *Biochem. Eng. J.*, 2009, **46**, 132–140.
10 M. Das, G. Sumana, R. Nagarajan and B. D. Malhotra, Zirconia based nucleic acid sensor for Mycobacterium tuberculosis detection, *Appl. Phys. Lett.*, 2010, **96**, 133703.
11 A. Abdussalam and B. G. Xu, Recent advances in electrochemiluminescence luminophores, *Anal. Bioanal. Chem.*, 2022, **414**, 131–146.
12 Y. T. Fu and Q. Ma, Recent developments of electrochemiluminescence nanosensor for cancer diagnosis applications, *Nanoscale*, 2020, **12**, 13879–13898.
13 Z. Zhang, P. Y. Du, G. Q. Pu, L. P. Wei, Y. X. Wu, J. N. Guo and X. Q. Lu, Utilization and prospects of electrochemiluminescence for characterization, sensing, imaging and devices, *Mater. Chem. Front.*, 2019, **3**, 2246–2257.
14 R. Zou, X. Teng, Y. J. Lin and C. Lu, Graphitic carbon nitride-based nanocomposites electrochemiluminescence systems and their applications in biosensors, *TrAC, Trends Anal. Chem.*, 2020, **132**, 116054.
15 Y. He, J. W. Du, J. H. Luo, S. H. Chen and R. Yuan, Coreactant-free electrochemiluminescence biosensor for the determination of organophosphorus pesticides, *Biosens. Bioelectron.*, 2020, **150**, 111898.
16 J. Adhikari, M. Rizwan, N. A. Keasberry and M. U. Ahmed, Current progresses and trends in carbon nanomaterials-based electrochemical and electrochemiluminescence biosensors, *J. Chin. Chem. Soc.*, 2020, **67**, 937–960.
17 H. M. Cao, X. Q. Hu, C. Y. Hu, Y. Zhang and N. Q. Jia, A novel solid-state electrochemiluminescence sensor for melamine with $Ru(bpy)_3^{2+}$/mesoporous silica nanospheres/nafion composite modified electrode, *Biosens. Bioelectron.*, 2013, **41**, 911–915.
18 T. Wang, S. Y. Zhang, C. J. Mao, J. M. Song, H. L. Niu, B. K. Jin and Y. P. Tian, Enhanced electrochemiluminescence of CdSe quantum dots composited with graphene oxide and chitosan for sensitive sensor, *Biosens. Bioelectron.*, 2012, **31**, 369–375.
19 Q. Wan, Q. Huang, M. Y. Liu, D. Z. Xu, H. Y. Huang, X. Y. Zhang and Y. Wei, Aggregation-induced emission active luminescent polymeric nanoparticles: non-covalent fabrication methodologies and biomedical applications, *Appl. Mater. Today*, 2017, **9**, 145–160.
20 J. D. Luo, Z. L. Xie, J. W. Lam, L. Cheng, H. Y. Chen, C. F. Qiu, H. S. Kwok, X. W. Zhan, Y. Q. Liu, D. B. Zhu and B. Z. Tang, Aggregation-induced emission of 1-methyl-1,2,3,4,5-pentaphenylsilole, *Chem. Commun.*, 2001, **18**, 1740–1741.
21 M. N. Huang, R. N. Yu, K. Xu, S. X. Ye, S. Kuang, X. H. Zhu and Y. Q. Wan, An arch-bridge-type fluorophore for bridging the gap between aggregation-caused quenching (ACQ) and aggregation-induced emission (AIE), *Chem. Sci.*, 2016, **7**, 4485–4491.
22 M. Chen, A. J. Qin, J. W. Y. Lam and B. Z. Tang, Multifaceted functionalities constructed from pyrazine-based AIEgen system, *Coord. Chem. Rev.*, 2020, **422**, 213472.
23 Y. C. Chen, J. W. Y. Lam, R. T. K. Kwok, B. Liu and B. Z. Tang, Aggregation-induced emission: fundamental understanding and future developments, *Mater. Horiz.*, 2019, **6**, 428–433.
24 S. Dalapati, C. Gu and D. L. Jiang, Luminescent porous polymers based on aggregation induced mechanism: design, synthesis and functions, *Small*, 2016, **12**, 6513–6527.
25 X. M. Huang, M. J. Lan, J. Wang, L. H. Guo, Z. Y. Lin, N. Sun, C. M. Wu and B. Qiu, A fluorescence signal amplification and specific energy transfer strategy for sensitive detection of β-galactosidase based on the effects of AIE and host-guest recognition, *Biosens. Bioelectron.*, 2020, **169**, 112655.
26 Y. J. Chen, H. J. Han, H. X. Tong, T. T. Chen, H. B. Wang, J. Ji and Q. Jin, Zwitterionic phosphorylcholine–TPE conjugate for pH-responsive drug delivery and AIE active imaging, *ACS Appl. Mater. Interfaces*, 2016, **8**, 21185–21192.
27 Q. Wan, G. J. Zeng, Z. Y. He, L. C. Mao, M. Y. Liu, H. Y. Huang, F. J. Deng, X. Y. Zhang and Y. Wei, Fabrication and biomedical applications of AIE active nanotheranostics through the combination of a ring-opening reaction and formation of dynamic hydrazones, *J. Mater. Chem. B*, 2016, **4**, 5692–5699.
28 X. Wei, M. J. Zhu, H. Yan, C. S. Lu and J. J. Xu, Recent advances in aggregation-induced electrochemiluminescence, *Chem. – Eur. J.*, 2019, **25**, 12671–12683.
29 S. Y. Ji, W. Zhao, H. Gao, J. B. Pan, C. H. Xu, Y. W. Quan, J. J. Xu and H. Y. Chen, Highly efficient aggregation-induced electrochemiluminescence of polyfluorene derivative nanoparticles containing tetraphenylethylene, *iScience*, 2020, **23**, 100774.
30 S. Carrara, A. Aliprandi, C. F. Hogan and L. D. Cola, Aggregation-induced electrochemiluminescence of platinum(II) complexes, *J. Am. Chem. Soc.*, 2017, **139**, 14605–14610.
31 K. Siddharth, P. Alam, M. D. Hossain, N. Xie, G. S. Nambafu, F. Rehman, J. W. Y. Lam, G. H. Chen, J. P. Cheng, Z. T. Luo, G. H. Chen, B. Z. Tang and M. H. Shao, Hydrazine detection during ammonia electro-

 This journal is © The Royal Society of Chemistry 2022

Published on 14 April 2022. Downloaded on 2/20/2026 8:42:33 PM.

oxidation using an aggregation-induced emission dye, *J. Am. Chem. Soc.*, 2021, **143**, 2433–2440.
32 Y. N. Hong, J. W. Y. Lam and B. Z. Tang, Aggregation-induced emission, *Chem. Soc. Rev.*, 2011, **40**, 5361–5388.
33 Y. J. Wang, J. Y. Nie, W. Fang, L. Yang, Q. L. Hu, Z. K. Wang, J. Z. Sun and B. Z. Tang, Sugar-based aggregation-induced emission luminogens: design, structures, and applications, *Chem. Rev.*, 2020, **120**, 4534–4577.
34 J. Mei, N. L. C. Leung and R. T. K. Kwok, Aggregation-induced emission: together we shine, united we soar, *Chem. Rev.*, 2015, **115**, 11718–11940.
35 G. H. Zhang, J. B. Sun, P. C. Xue, Z. Q. Zhang, G. Gong, J. Peng and R. Lu, Phenothiazine modified triphenylacrylonitrile derivates: AIE and mechanochromism tuned by molecular conformation, *J. Mater. Chem. C*, 2015, **3**, 2925–2932.
36 Q. H. Zhu, L. Huang, Z. P. Chen, S. C. Zheng, L. Y. Lv, Z. B. Zhu, D. R. Cao, H. F. Jiang and S. W. Liu, A new series of C-6 unsubstituted tetrahydropyrimidines: convenient one-pot chemoselective synthesis, aggregation-induced and size-independent emission characteristics, *Chem. – Eur. J.*, 2013, **19**, 1268–1280.
37 X. F. Fang, Y. M. Zhang, K. W. Chang, Z. H. Liu, X. Su, H. B. Chen, S. X. A. Zhang, Y. F. Liu and C. F. Wu, Facile synthesis, macroscopic separation, E/Z Isomerization, and distinct AIE properties of pure stereoisomers of an oxetane-substituted tetraphenylethene luminogen, *Chem. Mater.*, 2016, **28**, 6628–6636.
38 Q. L. Hu, M. Gao, G. X. Feng and B. Liu, Mitochondria-targeted cancer therapy using a light-up probe with aggregation-induced-emission characteristics, *Angew. Chem., Int. Ed.*, 2014, **53**, 1–6.
39 D. H. Wang, L. J. Chen, X. Zhao and X. P. Yan, Enhancing near-infrared AIE of photosensitizer with twisted intramolecular charge transfer characteristics via rotor effect for AIE imaging-guided photodynamic ablation of cancer cells, *Talanta*, 2021, **225**, 122046.
40 G. X. Feng, R. T. K. Kwok, B. Z. Tang and B. Liu, Functionality and versatility of aggregation-induced emission luminogens, *Appl. Phys. Rev.*, 2017, **4**, 021307.
41 R. R. Hu, J. L. Maldonado, M. Rodriguez, C. M. Deng, C. K. W. Jim, J. W. Y. Lam, M. M. F. Yuen, G. R. Ortiz and B. Z. Tang, Luminogenic materials constructed from tetraphenylethene building blocks: synthesis, aggregation-induced emission, two-photon absorption, light refraction, and explosive detection, *J. Mater. Chem.*, 2012, **22**, 232–240.
42 U. Caruso, B. Panunzi, R. Diana, S. Concilio, L. Sessa, R. Shikler, S. Nabha, A. Tuzi and S. Piotto, AIE/ACQ effects in two DR/NIR emitters: a structural and DFT comparative analysis, *Molecules*, 2018, **23**, 1947.
43 H. Q. Gao, X. Y. Zhang and C. Chen, Unity makes strength: how aggregation-induced emission luminogens advance the biomedical field, *Adv. Biosyst.*, 2018, **2**, 1800074.
44 Y. Liu, X. T. Tao, F. Z. Wang, X. N. Dang, D. C. Zou, Y. Ren and M. H. Jiang, Aggregation-induced emissions of fluorenonearylamine derivatives: a new kind of materials for nondoped red organic light-emitting diodes, *J. Phys. Chem. C*, 2008, **112**, 3975–3981.
45 D. Ding, K. Li, B. Liu and B. Z. Tang, Bioprobes based on AIE fluorogens, *Acc. Chem. Res.*, 2013, **46**, 2441–2453.
46 Y. Y. Yuan, D. Q. Wang, W. Long, F. J. Deng, S. X. Yu, J. W. Tian, H. Ouyang, S. Lin, X. Y. Zhang and Y. Wei, Ratiometric fluorescent detection of hypochlorite in aqueous solution and living cells using an ionic probe with aggregation-induced emission feature, *Sens. Actuators, B*, 2021, **330**, 129324.
47 R. R. Hu, N. L. C. Leung and B. Z. Tang, AIE macromolecules: syntheses, structures and functionalities, *Chem. Soc. Rev.*, 2014, **43**, 4494–4562.
48 N. B. Shustova, B. D. McCarthy and M. Dincă, Turn-on fluorescence in tetraphenylethylene-based metal–organic frameworks: an alternative to aggregation-induced emission, *J. Am. Chem. Soc.*, 2011, **133**, 20126–20129.
49 S. Dalapati, E. Jin, M. Addicoat, T. Heine and D. L. Jiang, Highly emissive covalent organic frameworks, *J. Am. Chem. Soc.*, 2016, **138**, 5797–5800.
50 Z. J. Qiu, S. T. Fan, C. Y. Xing, M. M. Song, Z. J. Nie, L. Xu, S. X. Zhang, L. Wang, S. Zhang and B. J. Li, Facile fabrication of an AIE-active metal–organic framework for sensitive detection of explosives in liquid and solid phases, *ACS Appl. Mater. Interfaces*, 2020, **12**, 55299–55307.
51 H. X. Liu, L. H. Xiong, R. T. K. Kwok, X. W. He, J. W. Y. Lam and B. Z. Tang, AIE bioconjugates for biomedical applications, *Adv. Opt. Mater.*, 2020, **8**, 2000162.
52 Y. Yu, Q. T. Gong, W. F. Lu, Y. H. Liu, Z. J. Yang, N. Wang and X. Q. Yu, Aggregation-induced emission probes for specific turn-on quantification of bovine serum albumin, *ACS Appl. Bio Mater.*, 2020, **3**, 5193–5201.
53 J. J. Pang, R. H. Du, X. Lian, Z. Q. Yao, J. Xu and X. H. Bu, Selective sensing of Cr^{VI} and Fe^{III} ions in aqueous solution by an exceptionally stable Tb^{III}-organic framework with an AIE-active ligand, *Chin. Chem. Lett.*, 2021, **32**, 2443–2447.
54 L. Tang, J. K. Jin, A. J. Qin, W. Z. Yuan, Y. Mao, J. Mei, J. Z. Sun and B. Z. Tang, A fluorescent thermometer operating in aggregation-induced emission mechanism: probing thermal transitions of PNIPAM in water, *Chem. Commun.*, 2009, **33**, 4974–4976.
55 Q. Zhang, Y. M. Zhang, H. Yao, T. B. Wei, B. B. Shi and Q. Lin, Supramolecular AIE polymer-based rare earth metallogels for the selective detection and high efficiency removal of cyanide and perchlorate, *Polym. Chem.*, 2021, **12**, 2001–2008.
56 D. H. Yuan, S. H. Chen, R. Yuan, J. J. Zhang and X. F. Liu, An ECL sensor for dopamine using reduced graphene oxide/multiwall carbon nanotubes/gold nanoparticles, *Sens. Actuators, B*, 2014, **191**, 415–420.
57 L. Fu, K. N. Fu, X. W. Gao, S. T. Dong, B. Zhang, S. J. Fu, H. Y. Hsu and G. Z. Zou, Enhanced near-infrared electro-

Published on 14 April 2022. Downloaded on 2/20/2026 8:42:33 PM.

chemiluminescence from trinary Ag–In–S to multinary Ag–Ga–In–S nanocrystals via doping-ingrowth and its immunosensing application, *Anal. Chem.*, 2021, **93**, 2160–2165.

58 Y. Huang, J. P. Lei, Y. Cheng and H. X. Ju, Ratiometric electrochemiluminescent strategy regulated by electrocatalysis of palladium nanocluster for immunosensing, *Biosens. Bioelectron.*, 2016, **77**, 733–739.

59 Y. P. Ding, X. Zhang, J. J. Peng, D. L. Zheng, X. S. Zhang, Y. B. Song, Y. W. Chen and W. H. Gao, Ultra-sensitive electrochemiluminescence platform based on magnetic metal-organic framework for the highly efficient enrichment, *Sens. Actuators, B*, 2020, **324**, 128700.

60 C. Ma, Y. Cao, X. D. Gou and J. J. Zhu, Recent progress in electrochemiluminescence sensing and imaging, *Anal. Chem.*, 2020, **92**, 431–454.

61 X. M. Shan, T. Pan, Y. T. Pan, W. C. Wang, X. H. Chen, X. L. Shan and Z. D. Chen, Highly sensitive and selective detection of Pb(II) by NH_2-SiO_2/$Ru(bpy)_3^{2+}$ UiO66 based solid-state ECL sensor, *Electroanalysis*, 2020, **32**, 462–469.

62 H. L. Qi, J. J. Teesdale, R. C. Pupillo, J. Rosenthal and A. J. Bard, Synthesis, electrochemistry, and electrogenerated chemiluminescence of two BODIPY-appended bipyridine homologues, *J. Am. Chem. Soc.*, 2013, **135**, 13558–13566.

63 Y. Namkoong, J. Oh and J. I. Hong, Electrochemiluminescent detection of glucose in human serum by BODIPY-based chemodosimeters for hydrogen peroxide using accelerated self-immolation of boronates, *Chem. Commun.*, 2020, **56**, 7577–7580.

64 J. Ma, W. J. Wang, Y. Li, Z. C. Lu, X. C. Tan and H. Y. Han, Novel porphyrin Zr metal–organic framework (PCN-224)-based ultrastable electrochemiluminescence system for PEDV sensing, *Anal. Chem.*, 2021, **93**, 2090–2096.

65 D. X. Du, J. N. Shu, M. Q. Guo, M. A. Haghighatbin, D. Yang, Z. P. Bian and C. H. Cui, Potential-resolved differential electrochemiluminescence immunosensor for cardiac troponin I based on MOF-5-wrapped CdS quantum dot nanoluminophores, *Anal. Chem.*, 2020, **92**, 14113–14121.

66 Y. G. Wang, G. H. Zhao, H. Chi, S. H. Yang, Q. F. Niu, D. Wu, W. Cao, T. D. Li, H. M. Ma and Q. Wei, Self-luminescent lanthanide metal–organic frameworks as signal probes in electrochemiluminescence immunoassay, *J. Am. Chem. Soc.*, 2021, **143**, 504–512.

67 H. Gao, N. Zhang, J. B. Pan, Y. W. Quan, Y. X. Cheng, H. Y. Chen and J. J. Xu, Aggregation-induced electrochemiluminescence of conjugated Pdots containing a trace Ir(III) complex: insights into structure–property relationships, *ACS Appl. Mater. Interfaces*, 2020, **12**, 54012–54019.

68 S. Carrara, B. Stringer, A. Shokouhi, P. Ramkissoon, J. Agugiaro, D. J. D. Wilson, P. J. Barnard and C. F. Hogan, Unusually strong electrochemiluminescence from iridium-based redox polymers immobilized as thin layers or polymer nanoparticles, *ACS Appl. Mater. Interfaces*, 2018, **10**, 37251–37257.

69 X. L. Huang, Q. Guo, R. Y. Zhang, Z. Zhao, Y. K. Leng, J. W. Y. Lam, Y. H. Xiong and B. Z. Tang, AIEgens: An emerging fluorescent sensing tool to aid food safety and quality control, *Compr. Rev. Food Sci. Food Saf.*, 2020, **19**, 1–33.

70 J. N. Guo, W. Q. Feng, P. Y. Du, R. Z. Zhang, J. Liu, Y. Liu, Z. M. Wang and X. Q. Lu, Aggregation-induced electrochemiluminescence of tetraphenylbenzosilole derivatives in an aqueous phase system for ultrasensitive detection of hexavalent chromium, *Anal. Chem.*, 2020, **92**, 14838–14845.

71 H. Jiang, Z. J. Qin, Y. K. Zheng, L. Liu and X. M. Wang, Aggregation-induced electrochemiluminescence by metal-binding protein responsive hydrogel scaffolds, *Small*, 2019, **15**, 1901170.

72 S. P. Li, J. Li, B. Geng, X. F. Yang, Z. L. Song, Z. J. Li, B. Y. Ding, J. Zhang, W. Y. Lin and M. Yan, TPE based electrochemiluminescence for ALP selective rapid one-step detection applied in vitro, *Microchem. J.*, 2021, **164**, 106041.

73 L. Yang, X. Sun, D. Wei, H. X. Ju, Y. Du, H. M. Ma and Q. Wei, Aggregation-induced electrochemiluminescence bioconjugates of apoferritin-encapsulated iridium(III) complexes for biosensing application, *Anal. Chem.*, 2021, **93**, 1553–1560.

74 Z. Y. Wang, J. B. Pan, Q. Li, Y. Zhou, S. Yang, J. J. Xu and D. B. Hua, Improved AIE-active probe with high sensitivity for accurate uranyl ion monitoring in the wild using portable electrochemiluminescence system for environmental applications, *Adv. Funct. Mater.*, 2020, **30**, 2000220.

75 R. T. K. Kwok, C. W. T. Leung, J. W. Y. Lam and B. Z. Tang, Biosensing by luminogens with aggregation induced emission characteristics, *Chem. Soc. Rev.*, 2015, **44**, 4228–4238.

76 W. Mani, T. Beduk, W. Khushaim, A. E. Ceylan, S. Timur, O. S. Wolfbeis and K. N. Salama, Electrochemical sensors targeting salivary biomarkers: a comprehensive review, *TrAC, Trends Anal. Chem.*, 2021, **135**, 116164.

77 J. M. Wang and B. Yan, Improving covalent organic frameworks fluorescence by triethylamine pinpoint surgery as selective biomarker sensor for diabetes mellitus diagnosis, *Anal. Chem.*, 2019, **91**, 13183–13190.

78 L. Farzin, S. Sadjadi, M. Shamsipur, A. Chabok and S. Sheibani, A sandwich-type electrochemical aptasensor for determination of MUC1 tumor marker based on PSMA-capped PFBT dots platform and high conductive RGO-N′1, N′3 -dihydroxymalonimidamide/thionine nanocomposite as a signal tag, *Electroanal. Chem.*, 2017, **807**, 108–118.

79 M. H. Jiang, S. K. Li, X. Zhong, W. B. Liang, Y. Q. Chai, Y. Zhuo and R. Yuan, Electrochemiluminescence enhanced by restriction of intramolecular motions (RIM): tetraphenylethylene microcrystals as a novel emitter for mucin 1 detection, *Anal. Chem.*, 2019, **91**, 3710–3716.

 This journal is © The Royal Society of Chemistry 2022

Published on 14 April 2022. Downloaded on 2/20/2026 8:42:33 PM.

80 W. Huang, G. B. Hu, L. Y. Yao, Y. Yang, W. B. Liang, R. Yuan and D. R. Xiao, Matrix coordination-induced electrochemiluminescence enhancement of tetraphenylethylene-based hafnium metal–organic framework: an electrochemiluminescence chromophore for ultrasensitive electrochemiluminescence sensor construction, *Anal. Chem.*, 2020, **92**, 3380–3387.

81 J. S. Li, H. Y. Jia, X. Ren, Y. Y. Li, L. Liu, R. Q. Feng, H. M. Ma and Q. Wei, Dumbbell plate-shaped AIEgen-based luminescent MOF with high quantum yield as self-enhanced ECL tags: mechanism insights and biosensing application, *Small*, 2022, **18**, 2106567.

82 J. W. Xue, L. Yang, Y. Du, Y. Ren, X. Ren, H. M. Ma, D. Wu, H. X. Ju, Y. Y. Li and Q. Wei, Electrochemiluminescence sensing platform based on functionalized poly-(styrene-co-maleicanhydride) nanocrystals and iron doped hydroxyapatite for CYFRA 21-1 immunoassay, *Sens. Actuators, B*, 2020, **321**, 128454.

83 M. Saremi, A. Amini and H. Heydari, An aptasensor for troponin I based on the aggregation-induce electrochemiluminescence of nanoparticles prepared from a cyclometallated iridium(III) complex and poly (4-vinylpyridine-co-styrene) deposited on nitrogen-doped graphene, *Microchim. Acta*, 2019, **186**, 254.

84 L. Cui, M. H. Zhao, C. C. Li, Q. B. Wang, X. L. Luo and C. Y. Zhang, A host–guest interaction-based and metal–-organic gel-based biosensor with aggregation-induced electrochemiluminescence enhancement for methyltransferase assay, *Anal. Chem.*, 2021, **93**, 2974–2981.

85 M. X. Yan, S. N. Feng, L. Y. Yu, Y. Xue, J. S. Huang and X. R. Yang, Label-free immunosensor for cardiac troponin I detection based on aggregation-induced electrochemiluminescence of a distyrylarylene derivative, *Biosens. Bioelectron.*, 2021, **192**, 113532.

86 L. Y. Yao, F. Yang, G. B. Hu, Y. Yang, W. Huang, W. B. Liang, R. Yuan and D. R. Xiao, Restriction of intramolecular motions (RIM) by metal-organic frameworks for electrochemiluminescence enhancement: 2D Zr12-adb nanoplate as a novel ECL tag for the construction of biosensing platform, *Biosens. Bioelectron.*, 2020, **155**, 112099.

87 N. N. Wang, Z. Y. Wang, L. Z. Chen, W. W. Chen, Y. W. Quan, Y. X. Cheng and H. X. Ju, Dual resonance energy transfer in triplecomponent polymer dots to enhance electrochemiluminescence for highly sensitive bioanalysis, *Chem. Sci.*, 2019, **10**, 6815–6820.

88 W. H. Zhou, M. Vazin, T. M. Yu, J. S. Ding and J. W. Liu, In vitro selection of chromium-dependent DNAzymes for sensing chromium(III) and chromium(VI), *Chem. – Eur. J.*, 2016, **22**, 9835–9840.

89 X. R. Yang, J. Xu, X. M. Tang, H. X. Liu and D. B. Tian, A novel electrochemical DNAzyme sensor for the amplified detection of Pb^{2+} ions, *Chem. Commun.*, 2010, **46**, 3107–3109.

90 E. Eftekhari, W. T. Wang, X. Li, A. Nikhil, Z. Q. Wu, R. Klein, I. S. Cole and Q. Li, Picomolar reversible Hg(II) solid-state sensor based on carbon dots in double heterostructure colloidal photonic crystals, *Sens. Actuators, B*, 2017, **240**, 204–211.

91 R. M. El-Shishtawy, H. A. A. Ghamdia, M. M. Alamc, Z. M. A. Amshanya, A. M. Asiria and M. M. Rahman, Development of Cd^{2+} sensor based on BZNA/nafion/glassy carbon electrode by electrochemical approach, *Chem. Eng. J.*, 2018, **352**, 225–231.

92 P. Alam, N. L. C. Leung, J. Zhang, R. T. K. Kwok, J. W. Y. Lam and B. Z. Tang, AIE-based luminescence probes for metal ion detection, *Coord. Chem. Rev.*, 2021, **429**, 213693.

93 Q. Zhang, P. Yang, J. X. Shen and J. H. Yu, Graphene-amplified photoelectric response of CdS nanoparticles for Cu^{2+} sensor, *J. Nanosci. Nanotechnol.*, 2019, **19**, 7871–7878.

94 Q. Han, C. Wang, Z. Z. Li, J. L. Wu, P. K. Liu, F. J. Mo and Y. Z. Fu, Multifunctional zinc oxide promotes electrochemiluminescence of porphyrin aggregates for ultrasensitive detection of copper ion, *Anal. Chem.*, 2020, **92**, 3324–3331.

95 Z. G. Han, Y. P. Zhang, Y. X. Wu, Z. M. Li, L. Bai, S. H. Huo and X. Q. Lu, Substituent-induced aggregated state electrochemiluminescence of tetraphenylethene derivatives, *Anal. Chem.*, 2019, **91**, 8676–8682.

96 F. Sun, Z. Y. Wang, Y. Q. Feng, Y. X. Cheng, H. X. Ju and Y. W. Quan, Electrochemiluminescent resonance energy transfer of polymer dots for aptasensing, *Biosens. Bioelectron.*, 2018, **100**, 28–34.

97 J. W. Zhao, J. H. Luo, D. Liu, Y. He, Q. Li, S. H. Chen and R. Yuan, A coreactant-free electrochemiluminescence (ECL) biosensor based on insitu generating quencher for the ultrasensitive detection of microRNA, *Sens. Actuators, B*, 2020, **316**, 128139.

98 Z. Q. Fan, Z. Q. Lin, Z. P. Wang, J. F. Wang, M. H. Xie, J. F. Zhao, K. Zhang and W. Huang, Dual-wavelength electrochemiluminescence ratiometric biosensor for NF-κB p50 detection with dimethylthiodiaminoterephthalate fluorophore and self-assembled DNA tetrahedron nanostructures probe, *ACS Appl. Mater. Interfaces*, 2020, **12**, 11409–11418.

99 L. P. Lu, L. L. Zhang, W. J. Miao, X. Y. Wang and G. S. Guo, Aggregation-induced electrochemiluminescence of the dichlorobis(1,10-phenanthroline)ruthenium (II) ($Ru(phen)_2Cl_2$)/Tri-n-propylamine (TPrA) system in H_2O–MeCN mixtures for identification of nucleic acids, *Anal. Chem.*, 2020, **92**, 9613–9619.

100 N. Zhang, H. Gao, Y. L. Jia, J. B. Pan, X. L. Luo, H. Y. Chen and J. J. Xu, Ultrasensitive nucleic acid assay based on AIE-active polymer dots with excellent electrochemiluminescence stability, *Anal. Chem.*, 2021, **93**, 6857–6864.

101 J. L. Zhang, Y. Yang, W. B. Liang, L. Y. Yao, R. Yuan and D. R. Xiao, Highly stable covalent organic framework nanosheets as a new generation of electrochemiluminescence emitters for ultrasensitive MicroRNA detection, *Anal. Chem.*, 2021, **93**, 3258–3265.

102 J. L. Liu, Y. Zhuo, Y. Q. Chai and R. Yuan, BSA stabilized tetraphenylethylene nanocrystals as aggregation induced

Published on 14 April 2022. Downloaded on 2/20/2026 8:42:33 PM.

enhanced electrochemiluminescence emitters for ultrasensitive microRNA assay, *Chem. Commun.*, 2019, **55**, 9959–9962.

103 O. E. Fayemi, A. S. Adekunle and E. E. Ebenso, Metal oxide nanoparticles/multi-walled carbon nanotube nanocomposite modified electrode for the detection of dopamine: comparative electrochemical study, *J. Biosens. Bioelectron.*, 2015, **6**, 1000190.

104 Y. L. T. Ngoa, P. L. Nguyen, W. M. Choi, J. S. Chung and S. H. Hu, Highly sensitive smartphone-integrated colorimetric glucose sensor based on $MnFe_2O_4$-graphitic carbon nitride hybrid nanostructure, *Mater. Res. Bull.*, 2020, **129**, 110910.

105 J. H. Guo, Uric acid monitoring with a smartphone as the electrochemical analyzer, *Anal. Chem.*, 2016, **88**, 11986–11989.

106 W. W. Yi, Z. P. Li, C. Dong, H. W. Li and J. F. Li, Electrochemical detection of chloramphenicol using palladium nanoparticles decorated reduced graphene oxide, *Microchem. J.*, 2019, **148**, 774–783.

107 S. H. Li, X. H. Ma, C. H. Pang, M. Y. Wang, G. H. Yin, Z. Xu, J. P. Li and J. H. Luo, Novel chloramphenicol sensor based on aggregation-induced electrochemiluminescence and nanozyme amplification, *Biosens. Bioelectron.*, 2021, **176**, 112944.

108 Z. H. Li, W. Qin and G. D. Liang, Mass-amplifying electrochemiluminescence film (MAEF) for visual detection of dopamine in aqueous media, *Nanoscale*, 2020, **12**, 8828–8835.

109 Z. Y. Wang, N. N. Wang, H. Gao, Y. W. Quan, H. X. Ju and Y. X. Cheng, Amplified electrochemiluminescence signals promoted by the AIE-active moiety of D–A type polymer dots for biosensing, *Analyst*, 2020, **145**, 233.

110 L. Cui, S. L. Yu, W. Q. Gao, X. M. Zhang, S. Y. Deng and C. Y. Zhang, Tetraphenylenthene-based conjugated microporous polymer for aggregation-induced electrochemiluminescence, *ACS Appl. Mater. Interfaces*, 2020, **12**, 7966–7973.

111 H. W. Liu, L. F. Wang, H. F. Gao, H. L. Qi, Q. Gao and C. X. Zhang, Aggregation-induced enhanced electrochemiluminescence from organic nanoparticles of donor–-acceptor based coumarin derivatives, *ACS Appl. Mater. Interfaces*, 2017, **9**, 44324–44331.

112 W. X. Lv, Q. T. Yang, Q. Li, H. Y. Li and F. Li, Quaternary ammonium salt-functionalized tetraphenylethene derivative boosts electrochemiluminescence for highly sensitive aqueous-phase biosensing, *Anal. Chem.*, 2020, **92**, 11747–11754.

113 X. H. Xiong, Y. F. Li, W. Yuan, Y. C. Lu, X. Xiong, Y. Li, X. Y. Chen and Y. J. Liu, Screen printed bipolar electrode for sensitive electrochemiluminescence detection of aflatoxin B1 in agricultural products, *Biosens. Bioelectron.*, 2020, **150**, 111873.

114 X. Y. Lv, X. Y. Xu, T. Miao, X. F. Zang, C. Geng, Y. P. Li, B. Cui and Y. S. Fang, Aggregation-induced electrochemiluminescence immunosensor based on 9,10-diphenylanthracene cubic nanoparticles for ultrasensitive detection of aflatoxin B1, *ACS Appl. Bio Mater.*, 2020, **3**, 8933–8942.

115 Z. Y. Wang, M. Y. Xu, N. Zhang, J. B. Pan, X. Q. Wu, P. Liu, J. J. Xu and D. B. Hua, An ultra-highly sensitive and selective self-enhanced AIECL sensor for public security early warning in a nuclear emergency via a co-reactive group poisoning mechanism, *J. Mater. Chem. A*, 2021, **9**, 12584.

116 L. Cui, J. H. Zhou, C. C. Li, S. Y. Deng, W. Q. Gao, X. M. Zhang, X. L. Luo, X. L. Wang and C. Y. Zhang, Bipolar aggregation-induced electrochemiluminescence of thiophene-fused conjugated microporous polymers, *ACS Appl. Mater. Interfaces*, 2021, **13**, 28782–28789.

117 Z. G. Han, Z. F. Yang, H. S. Sun, Y. L. Xu, X. F. Ma, D. L. Shan, J. Chen, S. H. Huo, Z. Zhang, P. Y. Du and X. Q. Lu, Electrochemiluminescence platforms based on small water-insoluble organic molecules for ultrasensitive aqueous-phase detection, *Angew. Chem., Int. Ed.*, 2019, **58**, 5915–5919.

118 J. L. Yang, J. M. Wei, F. Luo, J. Dai, J. J. Hu, X. D. Lou and F. Xia, Enzyme-responsive peptide-based AIE bioprobes, *Top. Curr. Chem.*, 2020, **378**, 47.

 This journal is © The Royal Society of Chemistry 2022